



VCU

Virginia Commonwealth University
VCU Scholars Compass

Theses and Dissertations


Graduate School

2017

DEVELOPMENT OF AN ELECTROSPUN AND 3D PRINTED CELLULAR DELIVERY DEVICE FOR DERMAL WOUND HEALING

Ryan M. Clohessy
Virginia Commonwealth University

Follow this and additional works at: <https://scholarscompass.vcu.edu/etd>

 Part of the [Biomaterials Commons](#), [Biomedical Devices and Instrumentation Commons](#), and the [Molecular, Cellular, and Tissue Engineering Commons](#)

© Ryan Clohessy

Downloaded from

<https://scholarscompass.vcu.edu/etd/6026>

This Dissertation is brought to you for free and open access by the Graduate School at VCU Scholars Compass. It has been accepted for inclusion in Theses and Dissertations by an authorized administrator of VCU Scholars Compass. For more information, please contact libcompass@vcu.edu.

© Ryan M. Clohessy 2019

All Rights Reserved

DEVELOPMENT OF AN ELECTROSPUN AND 3D PRINTED CELLULAR DELIVERY
DEVICE FOR DERMAL WOUND HEALING

A dissertation submitted in partial fulfillment of the requirements for the degree of Doctor
of Philosophy in Biomedical Engineering at Virginia Commonwealth University.

By

Ryan Matthew Clohessy

Bachelor of Science in Biomedical Engineering, University of Virginia, 2007

Advisor: Zvi Schwartz, D.M.D., Ph.D.

Associate Dean for Strategic Initiatives

Professor, Department of Biomedical Engineering

Virginia Commonwealth University

Richmond, Virginia

June 2019

iii

ACKNOWLEDGEMENTS

There are many people I would like to thank for their support, encouragement, and guidance; without each of you, I certainly would not be where I am today. I first would like to thank Dr. Schwartz and Dean Boyan; you have provided me with unbelievable support, incredible experiences and a true lab family to call my own. I will never forget the opportunities you generously gave, nor the encouragement and direction you provided, especially when I needed it most. More than the knowledge you've imparted, you have helped me become a better version of myself.

To my committee members, Dr. Lemmon, Dr. Tang, Dr. Yadavalli, and Dr. Yang; thank you for being on my committee. From lab space and equipment to advice and direction, thank you; I have truly enjoyed working with you and am honored to have you as my mentors.

To my friends, in Richmond and elsewhere, thank you for your support and encouragement. It has been a blessing to have you in my life, and I will never forget the memories we have made. You will always have a place in my heart.

To my family, especially my parents John and Lois, thank you for your never-ending love and unwavering support. You have encouraged me to pursue my goals and stood by me every step of the way. This would not have been possible without you and I am lucky to have you as my parents.

Last, but not least, thank you to my wife Stephanie. You believed in me and encouraged me, even when I did not believe in myself. Your love (and patience) was what kept me going and continues to make everything worthwhile. Thank you for always making me smile, keeping me sane through the sleepless nights and tolerating me through my most stressful moments. **I love you all the way.**

TABLE OF CONTENTS

ACKNOWLEDGMENTS	iv
LIST OF FIGURES AND TABLES.....	vii
LIST OF SYMBOLS AND ABBREVIATIONS	ix
ABSTRACT	1
CHAPTER	
1 BACKGROUND AND LITTERATURE REVIEW.....	2
Wound Healing and Regeneration.....	2
Tissue Engineering of Skin	4
Polyglycolic Acid	6
Poly-Ethylene Glycol.....	7
Polyvinyl Alcohol	7
3D Printing	8
Electrospinning	8
2 DEVELOPMENT OF AN BIODEGRADABLE THREE-DIMENSIONAL CELL DELIVERY BANDAGE	10
Introduction	12
Materials and Methods	14
Results	22
Discussion.....	28
Conclusion	32
References.....	34
3 IN VIVO EVALUATION OF AN ELECTROSPUN AND 3D PRINTED CELLULAR DELIVERY DEVICE FOR DERMAL WOUND HEALING	37
Introduction	39
Materials and Methods	41
Results	48

Discussion.....	56
Conclusion	58
References.....	60
4 CONCLUSIONS	65
REFERENCES (CHAPTER 1)	68

LIST OF FIGURES AND TABLES

Figure 1: Phases of the Wound Healing Cycle.....	3
Figure 2: The Structure of Human Skin.....	5
Figure 3: Chemical Structure of Polyglycolic Acid.....	7
Figure 4: Chemical Structure of Polyethylene Glycol.....	7
Figure 5: Chemical Structure of Polyvinyl Alcohol.....	8
Figure 6: Figure 1: Schematic of Fabrication Process with Photographs of Construct .	15
Figure 7: Figure 2: Table of Polymer Solutions and SEM image of Electrospun Fibers	16
Figure 8: Figure 3: PVA Dissolution	17
Figure 9: Figure 4: SEM Images of Fibers Before and After PVA Wash-out.....	18
Figure 10: Figure 5: Electrospun Fiber Characterization.....	24
Figure 11: Figure 6: Response of hMSCs to Construct Degradation Byproducts	25
Figure 12: Figure 7: hMSC Response to Culture Within the Construct.....	27
Figure 13: Figure 8: MSCs Retain Ability to Differentiate Within Construct	28
Figure 14: Figure 1: Schematic of Fabrication Process with Photographs of Construct	41
Figure 15: Figure 2: Results of <i>In Vivo</i> Study #1	48
Figure 16: Figure 3: Representative Histological Images of <i>In Vivo</i> Study #1	50
Figure 17: Figure 4: Results of <i>In Vivo</i> Study #2.....	52
Figure 18: Figure 5: Representative Histological Images of <i>In Vivo</i> Study #2	53
Figure 19: Figure 6: Average Blood Vessel Counts of <i>In Vivo</i> Study #2	54

LIST OF SYMBOLS AND ABBREVIATIONS

PVA

PEG

VEGF

BMP-2

FGF

PGA

ECM

G

HFP or HFIP

FDA

PCL

μ

MSC

SEM

PBS

ATR-FTIR

P

MSCGM

TCPS

CM

DNA

ELISA

IACUC

ASC

STP

H&E

EDTA

ANOVA

α -SMA

PLGA

BMSC

MG63

ASTM

CT

ABSTRACT

DEVELOPMENT OF AN ELECTROSPUN AND 3D PRINTED CELLULAR DELIVERY DEVICE FOR DERMAL WOUND HEALING

By

Ryan M. Clohessy, B.S.

A dissertation submitted in partial fulfillment of the requirements for the degree
Doctor of Philosophy at
Virginia Commonwealth University 2017.

Advisor: Zvi Schwartz, D.M.D., Ph.D., Associate Dean for Strategic Initiatives,
Professor, Department of Biomedical Engineering, Virginia Commonwealth University

The goal of this research was to develop a system of individualized medicine that could be applied to dermal wounds serving as a wound dressing and synthetic extracellular matrix while delivering stem cells to the wound bed. First, fabrication parameters for electrospinning polymer fibers were determined. This involved evaluating fiber morphology with respect to polymer selection and solution concentration. Next, construct fabrication was examined to produce an integrated void space, or cargo area, suitable to maintain stem cells. *In vitro* studies to ensure stem cell viability and phenotype were conducted, and results supported the notion that cells could be administered to the wound site through construct pre-seeding. Lastly, *in vivo* studies were conducted to evaluate the construct as an applied biomaterial and as a cellular delivery device. Wound closure and quality were assessed, and neo-vascularization quantified. This project will provide insight into the tissue engineering field regarding cell-based therapies and dermal wound healing.

CHAPTER 1

Background and Literature Review

Wound Healing and Regeneration

Wounds are described as a defect or break in the skin resulting from physical or thermal damage or as a result of the presence of an underlying medical or physiological condition [4]. Normal wound healing is a process with four overlapping phases: Hemostasis and Inflammation, Migratory, Proliferative, and Remodeling. Bleeding usually occurs when the skin becomes damaged and flushes bacteria and antigens from the wound site. The clotting cascade, a sequence of clotting factor activation forms a fibrin plug to stop the bleeding. This clot provides hemostasis and occurs as the inflammation stage begins. Vasodilation occurs as a response to histamine and serotonin [4] which allows phagocytes to enter the wound and begin digesting necrotic tissue. The migratory phase occurs when fibroblasts and epithelial cells are recruited to the wound and begin to replace lost or damaged tissue. The proliferation phase begins with or immediately after the migratory phase. In this phase, granulation tissue is formed while blood and lymphatic vessels grow into the wound. Collagen matrix production is increased and lends to the strength and shape of the new skin. Finally, the remodeling, or maturation phase, occurring several weeks up to two years, strengthens the new epithelium and forms additional cellular connective tissue and matrices[5].

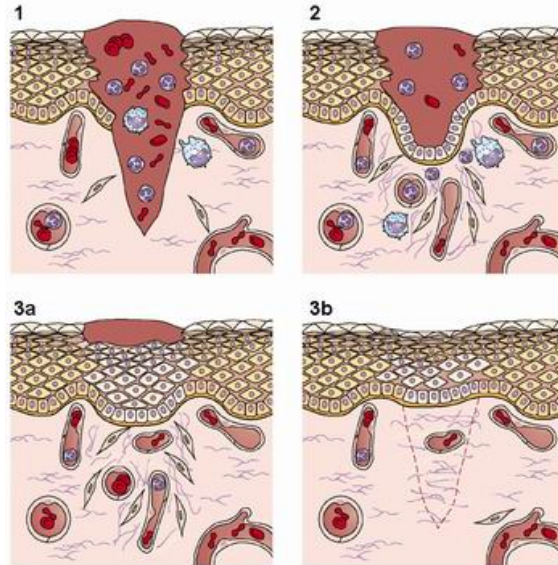


Figure 1: Phases of the wound healing cycle: 1. Inflammatory Phase 2. Migratory Phase 3a. Proliferative Phase 3b. Remodeling Phase [4].

Regeneration is typically a process that occurs when the wound is superficial and the original tissue can be exactly restored. When the wound is deeper, impacting the dermis, regeneration is not possible and wounds are closed through repair, usually resulting in scar tissue [6]. Generally, wounds which are able to re-epithelialize within 2 weeks do not form scars as minimal collagen is deposited. However, wounds which do not become covered with epithelial tissue within this time form scars as excess collagen builds up. The excess collagen fibers have a pronounced alignment which results in inferior functional quality to the random alignment of normal tissue.

Wounds that do not heal within expected timeframes are considered chronic wounds. These wounds have had the healing process interrupted at one or more stages and are the focus of the work herein. Chronic wounds may be a result of a patients' underlying condition or an outside influence such as a pathogenic bacterial infection. In either case, chronic wounds need additional influences and support to be jump started

back into the wound healing process. Clinically, this will often be accomplished with a graft to support the wound bed and help reestablish the lost tissue.

The focus of this research proposal will be on engineering a construct that supports host cell ingrowth, and is able to deliver a cellular payload, specifically stem cells, and their secreted soluble factors such as VEGF, BMP2, and FGF. Designed to supplement or replace tissue grafting and support wound healing, the construct developed herein will support both 'fresh' and chronic wounds and promote regeneration.

Tissue Engineering of Skin

Tissue engineering is the development of native tissue substitutes that are able to repair and regenerate damaged tissue to return natural function and state [7]. Skin, the largest organ of the human body, functions to protect against environmental hazards. Safeguarding the internal milieu from instability, life cannot be sustained without it. Tissue engineering of skin is a complicated process as skin is composed of three layers, the epidermis, basement membrane, and the dermis, which together provide for the skin's functions. The epidermis is composed primarily of keratinocytes and is separated from the dermis by the basement membrane but functionally connects both layers. The dermis contains the extracellular matrix composed of collagen, reticulum fibers, elastin and glycosaminoglycans, and is primarily populated by fibroblasts [8].

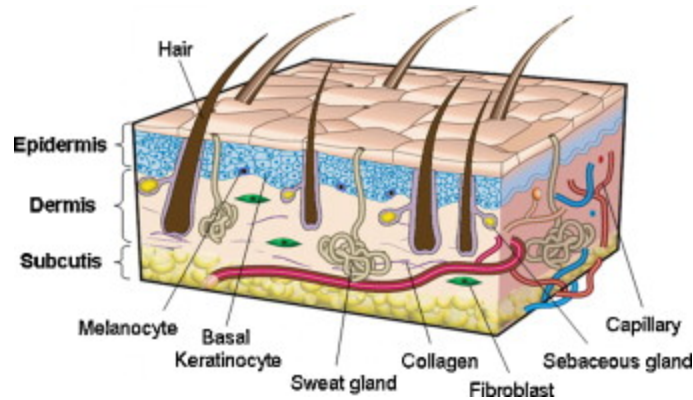


Figure 2: The Structure of Human Skin [2].

Historically, complex wounds requiring more than bandages or dressings have been treated with autografts, allografts, or xenografts. Autografts are skin grafts, or layers of skin that have been harvested from elsewhere on the patient's body and are transplanted onto the wound site. Currently, this technique is the 'gold standard' as there is no risk of disease transmission and the possibility of rejection is minimized as the tissue is the patient's own. Allografts are skin grafts taken from a donor. Usually cadaveric in origin, these grafts have the potential to transmit disease from donor to patient, as well as be rejected by the patient through an immune response. The last type of graft is a xenograft. Xenografts are animal derived grafts, generally porcine, and are usually irradiated or treated to help prevent xenogeneic cells from transmitting diseases or eliciting an immune response. Xenografts are generally used as a temporary graft or covering until an autograft or appropriate alternative can be implemented.

Recently, research has been focused on synthetic skin grafts and skin substitutes. These may be cellular or acellular and often incorporate antimicrobials, growth factors, or supplements [4]. Acellular grafts are made from synthetic collagen and hyaluronic acid or are cultured sheets that have been decellularized, preserving the dermal shape and

matrix properties. Cellular grafts are generally biodegradable films which have been loaded with autologous or recombinant skin cells [9]. Recently cultured epidermal autografts have been extensively studied, with six cellular synthetic grafts commercially available. An ideal skin substitute would improve on each of these current techniques and possess the following characteristics: inexpensive, analgesic, long shelf life, be used off the shelf, non-antigenic, durable, flexible, prevent water loss, antimicrobial, conform to irregular wounds, easy to secure, grow with children, and able to be applied in a single operation.

Polyglycolic Acid (PGA)

Polymer selection plays a critical role in designing a scaffold for tissue engineering. The polymer must meet certain criteria such that the scaffold is nontoxic, biocompatible, biodegradable, and does not illicit a severe immune response. The polymer of choice should also have a predictable degradation pattern as well as a quantifiable drug/protein release profile. Polyglycolic acid is a biodegradable polymer and the simplest linear, aliphatic polyester. It is known to be biocompatible, nontoxic, and degrades to glycolic acid monomers [25, 26]. The buildup of protons will reduce the pH of the wound microenvironment and may be a pro-angiogenic influence [10]. The byproducts of degradation can be processed by the body through the tricarboxylic acid cycle and excreted as water and carbon dioxide, with remaining parts excreted through urine. Commonly used in resorbable sutures, PGA has a proven track record in the biomedical community [26]. PGA used in this study was PGA 100 from Lakeshore Biomedical/Evonik (Birmingham, AL, USA).

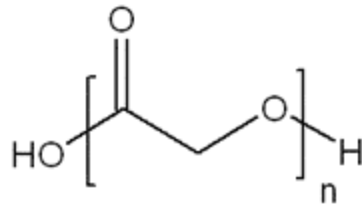


Figure 3: Chemical structure of polyglycolic acid.

Poly-Ethylene Glycol (PEG)

Poly-ethylene glycol is a water-soluble polymer which, when added to the polymer solution, acts as a stabilizer and can ease the electrospinning processing [28]. This occurs by modifying the viscosity of the polymer solution. The addition of PEG also aids in manipulating the degradation rate of the scaffold as it increases the water uptake of the polymer blend thus increasing the rate of degradation [11]. Lastly, PEG can also improve the hydrophilicity of PGA scaffolds [28]. PEG used in this study was from Fluka, Polyethylene Glycol 20,000 (MW).

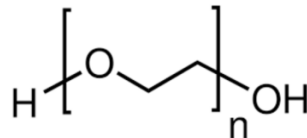


Figure 4: Chemical structure of polyethylene glycol.

Polyvinyl Alcohol (PVA)

Polyvinyl alcohol is generally regarded as safe, biocompatible and is used in many biomaterials [12, 27]. It is water soluble and available in 3D printer filament making it an ideal material choice to form the void fillers (as 3D printed PVA dissolves in static water within four hours). PVA used here is undyed, natural color from UltiMachine in 1.75mm diameter filament on a 1kg spool (South Pittsburg, TN, USA).

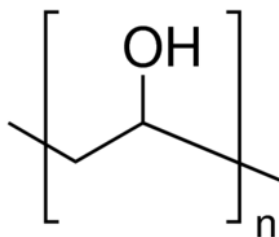


Figure 5: Chemical structure of polyvinyl alcohol.

3D Printing

3D printing of the void space templates was done using a MakerBot X2 printer (New York, New York, USA). The printer head is able to control extrusion temperature, bed temperature, print speed, and layer height. For template printing, we used an extrusion temperature of 190°C onto an unheated print bed, with a print speed of 90mm/sec and layer height of 0.1mm. Void templates were constructed in three pieces to allow for layer-by-layer fabrication and electrospun fiber deposition between each level.

Electrospinning

Electrospun polymeric scaffolds are non-woven fibrous meshes with fiber diameters on the order of microns. Scaffolds can be designed to various thicknesses and cut to match size and shape needs. Tailoring of the polymer solution can regulate the degradation rate. These characteristics are greatly affected by the high surface area to volume ratio fibrous scaffolds possess over solids. Electrospinning is preferable to woven materials because the seemingly random orientation of the fibers more closely matches that of the ECM. Scaffolds were electrospun through a Becton Dickenson 18G 1" blunt tip needle, fed via a KD Scientific Variable Syringe Pump. The polymer solution will be charged using a Spellman CZE 1000 R high voltage power supply and collected on a grounded target. Solution feed rates, voltages, and distance were tailored to produce a

scaffold with optimal characteristics. Scaffolds for this study are formed by dissolving the polymer blend in hexafluoroisopropanol (HFP) by TCI America (1,1,1,3,3,3 Hexafluoro-2 propanol).

CHAPTER 2
DEVELOPMENT OF A BIODEGRADABLE THREE-DIMENSIONAL CELL DELIVERY
BANDAGE

Authors: Ryan M Clohessy¹, Karolina Stumbraite¹, Barbara D Boyan^{1,2}, Zvi Schwartz^{1,3}

Affiliations: ¹Department of Biomedical Engineering, Virginia Commonwealth University, Richmond, VA, United States; ²Wallace H. Coulter Department of Biomedical Engineering, Georgia Institute of Technology, Atlanta, GA, United States; ³Department of Periodontics, University of Texas Health Science Center at San Antonio, San Antonio, TX, United States

Corresponding Author:

Barbara D. Boyan, Ph.D.
College of Engineering
Virginia Commonwealth University
601 West Main Street, Suite 331
Richmond, Virginia 23284
bboyan@vcu.edu

Running Title: Biodegradable 3D bandage

Keywords: electrospinning; 3D printing; polyglycolic acid; polyethylene glycol; polyvinyl alcohol; resorbable; mesenchymal stem cell delivery

Abstract

Cell-based therapies have garnered significant attention in recent years. As a treatment, the therapeutic effectiveness of the cells is often directly correlated to their ability to remain at the target locale. In an effort to provide localized delivery, we have developed a resorbable “bandage” shaped construct with the ability to deliver a payload of cells to the treatment site. To do this, a blend of polyglycolic acid (PGA) and polyethylene glycol (PEG) was electrospun as part of a custom fabrication method that incorporated 3D printed polyvinyl alcohol (PVA) sacrificial elements. Electrospun fibers were $0.55\mu\text{m}$ ($\pm 0.2\mu\text{m}$), creating a non-woven mesh with pore size of $3.8\mu\text{m}^2$ ($\pm 2.7\mu\text{m}^2$). This preparation is unique compared to traditional electrospinning as the sacrificial elements produce an internal void space for an injectable payload, which may be delivered to the target site. Human mesenchymal stem cells (hMSCs) incorporated into the scaffold maintained their ability to differentiate while remaining viable over 10 days in culture. Taking advantage of this ability may prove beneficial in regeneration, particularly in challenged or compromised wounds.

1. Introduction

Tissue engineering approaches for regenerative medicine, such as acellular grafts made of collagen or hyaluronic acid, or decellularized tissue matrices, have gained popularity in recent years.¹⁻³ Synthetic cellular grafts made of biodegradable films cultured with autologous, allogeneic or genetically-modified cells have also begun to be made commercially available.⁴ Although the use of engineered grafts is a step forward in regenerative medicine applications, these grafts experience some of the drawbacks of conventional grafts, such as a high risk of rejection, transmission of infection, excess scarring, and expense to the patient and care providers.⁵ Delivery of autologous cells has mitigated some of the drawbacks but their effectiveness often depends on the delivery method used. Synthetic scaffolds can reduce the risk of rejection, especially when used with autologous cells, putting these technologies at the forefront of medical engineering. Therefore, there is a great need for a biodegradable, synthetic, off-the-shelf materials that can deliver a cellular payload.

Electrospinning is a versatile process that can produce micro- to nano-sized fibers from a polymer solution that can closely mimic the extracellular matrix.^{6, 7} We applied this technique to produce a randomly oriented microfiber scaffold from two polymers, poly(glycolic acid) (PGA) and poly(ethylene glycol) (PEG), and used polyvinyl alcohol (PVA) to create a void space pocket for a payload of cells or therapeutic agents. These components were selected because of their individual attributes. PGA is a biodegradable polymer that is found most commonly in resorbable surgical sutures. PGA scaffolds can support a variety of cells⁸⁻¹⁰. However, during degradation, they can also result in an acidic microenvironment at the wound site¹¹, which may encourage angiogenesis.¹² PEG is a

water-soluble polymer that facilitates more uniform electrospun fibers, as well as allowing modification of fiber degradation.¹³ PVA is 3D printed into sacrificial elements that are removed prior to clinical use. By incorporating it into the device as a spacer, we were able to generate a three dimensional (3D) “bandage” construct.

The randomly oriented fibers of the scaffold allow native cells from the treatment site to attach and proliferate into the 3D environment created by the fiber mesh, contributing to the healing and remodeling processes.¹⁴ By incorporating an internal void space, a payload can be delivered to the target location. Using 3D printing together with an appropriate void space filler, nearly limitless configurations of the cargo area can be designed and included within the construct. Here we chose a 1cm x 1cm square template as this resulted in a construct that nicely fit a 12-well plate for in vitro testing. The payload can consist of cells, bioactive factors, or combinations of agents. We selected human mesenchymal stem cells (MSCs) as the payload, based on observations that addition of MSCs to wound sites has been noted to improve healing and regeneration outcomes.¹⁵⁻

18

The aim of this study was to develop a better bandage; namely, a resorbable wound dressing that could deliver and localize a payload of cells while serving as a matrix for host cell ingrowth. To achieve our aim, we first developed a design to provide both an enclosed volume for a cellular payload and sufficient surface area to allow the cells to adhere. We next optimized the polymer solution and electrospinning parameters and characterized the construct to determine the fiber diameter and pore size of the microfiber component. The completed construct was then assessed for its degradation rate and

suitability for cell growth. Finally, the construct was evaluated for any influences it might have on cell behavior.

2. Materials and methods

2.1 Overview of construct fabrication

Final constructs were fabricated using a combination of techniques, which are described briefly here and shown in Figure 1A. Sub-micron fibers were vertically electrospun onto a flat aluminum foil target. Layers of electrospun fibers were alternated with 3D printed 'void templates' until a seven-layer construct was complete. Before positioning the second and third layers of 3D printed sacrificial elements, small cuts were made in the covering electrospun fiber layer. This allowed contact between sacrificial elements along two parallel edges, thereby forming an interconnected "reservoir." The completed constructs were air-dried in a vacuum desiccator prior to removing the sacrificial elements. After washing out the PVA, the final construct had an interconnected void within the electrospun fibers (Figures 1B,C). The appearance of an 'as-fabricated' construct can be seen in Figure 1C with an exploded view highlighting the internal, interconnected PVA sacrificial elements interpolated with electrospun fibers (red arrows). Constructs were sterilized by soaking in 70% ethanol for 1 h followed by three five-minute rinses in sterile PBS under aseptic conditions.

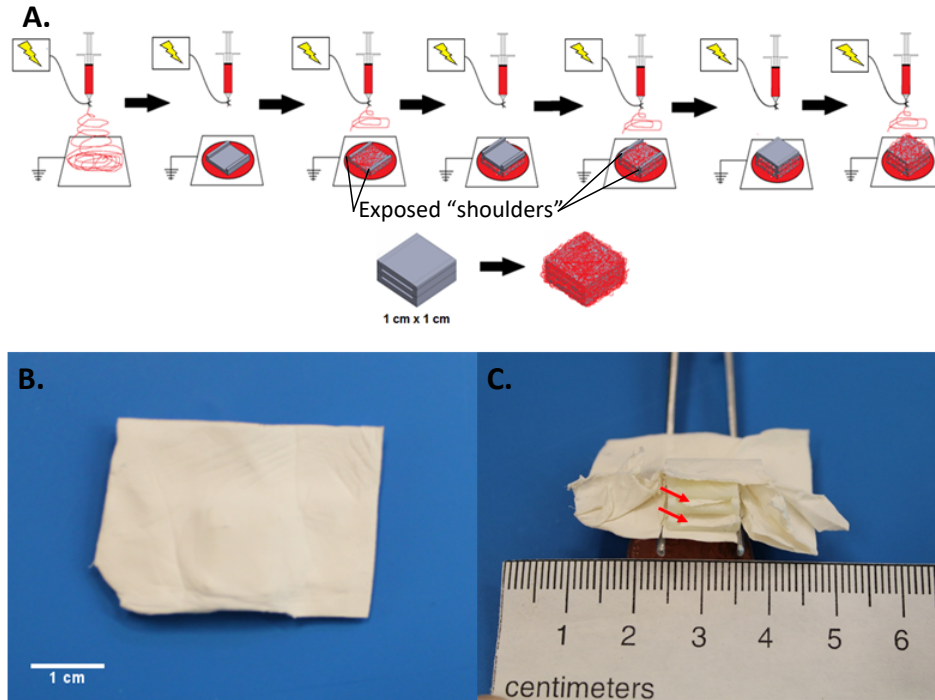


Figure 1: Schematic of fabrication process (A). Photograph of construct as-fabricated (B) and bisected to reveal internal composition (C). Arrows in (C) point to layers of electrospun fibers between the PVA sacrificial elements.

2.2 Electrospinning

Electrospun scaffolds can be designed to various thicknesses and cut to match size and shape needs. Tailoring of the polymer solution can regulate the degradation rate, often faster due to the high surface area to volume ratio fibrous scaffolds possess versus bulk solids. In addition, electrospinning is preferable to woven materials because the seemingly random orientation of the fibers more closely matches that of the extracellular matrix (ECM).¹⁹

To make the constructs in the present study, scaffolds were electrospun through a Becton Dickinson 18G 1" blunt tip needle, fed via a KD Scientific Variable Syringe Pump. The polymer solution was charged using a Spellman CZE 1000 R high voltage power supply and collected on a grounded target. Solution composition, feed rates,

voltages, and distance were tailored to produce a scaffold with optimal characteristics defined as smooth and uniform fibers. Multiple polymer blends and parameters were tested to down select to the final formulation (Figure 2), which was 140:40 PGA:PEG (w:w). Scaffolds for this study were formed by dissolving the polymer blend of polyglycolic acid (PGA, i.v. 1.0-2.0, Polysciences Inc., Warrington, PA) and polyethylene glycol (PEG, Mw=20,000, Sigma Aldrich, St. Louis, MO) in 1,1,1,3,3,3 hexafluoro-2 propanol (HFP) (TCI America, Portland, OR).

Trial #	Solution Concentration	Consistent Fibers (Yes/No)
1	100 mg/mL PCL	Yes
2	150 mg/mL PCL	Yes
3	100 mg/mL PGA	No
4	150 mg/mL PGA	No
5	200 mg/mL PGA	No
6	80:40 PGA:PEG wt:wt (net: 120 mg/mL)	No
7	80:60 PGA:PEG wt:wt (net: 140 mg/mL)	No
8	140:40 PGA:PEG wt:wt (net: 180 mg/mL)	Yes
9	150:50 PGA:PEG wt:wt (net: 200 mg/mL)	Yes
10	200:50 PGA:PEG wt:wt (net: 250 mg/mL)	No

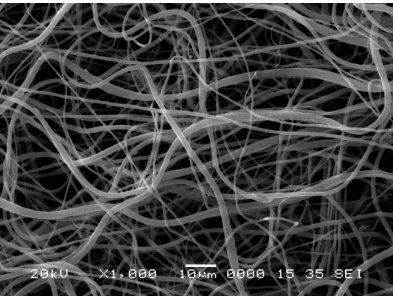


Figure 2: Table of polymer solutions tested (left). Scanning electron microscope image (right) of fibers produced from down-selected solution 140:40 mg/mL PGA:PEG. 1000x

2.3 3D Printing

2.3.1 PVA Sacrificial Elements

3D printing of the void space templates was done using a MakerBot X2 printer (New York, New York, USA). The printer head is able to control extrusion temperature, bed temperature, print speed, and layer height. PVA was selected as the appropriate void filler polymer as it is water soluble and available in a 3D printer filament. For template printing, we used an extrusion temperature of 190°C onto an unheated print bed, with a print speed of 90mm/sec and layer height of 0.1mm. Void templates were constructed in three pieces to allow layer-by-layer fabrication and designed for interconnection and electrospun fiber deposition between each level. These void templates were printed from

1.75mm diameter PVA filament (Ultimachine, South Pittsburgh, TN) and evaluated for dissolution rate through observation in static conditions over time. Additionally, we needed to ensure that the PVA be cleanly removed from a completed construct.

2.3.2 PVA Dissolution

Prior to PVA dissolution, the constructs were dried in a vacuum desiccator for a minimum of 24 hours, where they remained until used. In order to determine the optimal parameters for PVA dissolution, samples of the void fillers that were printed 5x larger than the PVA void fillers used in the bandage were assessed for dissolution over time in static de-ionized water under ambient conditions (Figure 3A). The time course of dissolution was determined using these PVA constructs; samples were incubated as above for 30, 60, 90, 120, 150, 180, and 240 minutes (Figure 3B).

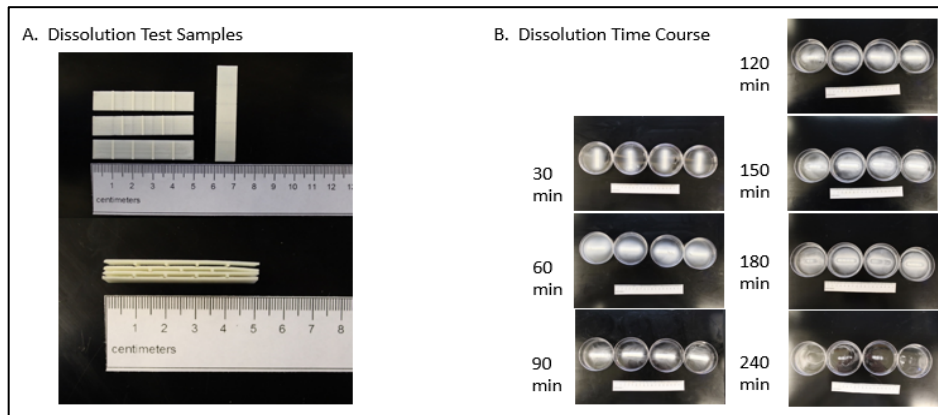


Figure 3: PVA dissolution. Test samples were 3D-printed 5x size (A). Change in construct morphology in deionized water under static conditions at ambient temperatures with water exchanges at every 30 min.

To ensure PVA washout from the finished constructs (PGA/PEG polymer + PVA void filler), each batch of 18 constructs was incubated at room temperature overnight in 4L of de-ionized water. To ensure PVA was completely removed from the bandage, SEM images were taken before and after the wash-out. Figure 4 displays the lack of

differences between fiber sheets before and after wash-out procedure, indicating that the PVA was fully washed out and did not result in any residue build up or particulate remains.

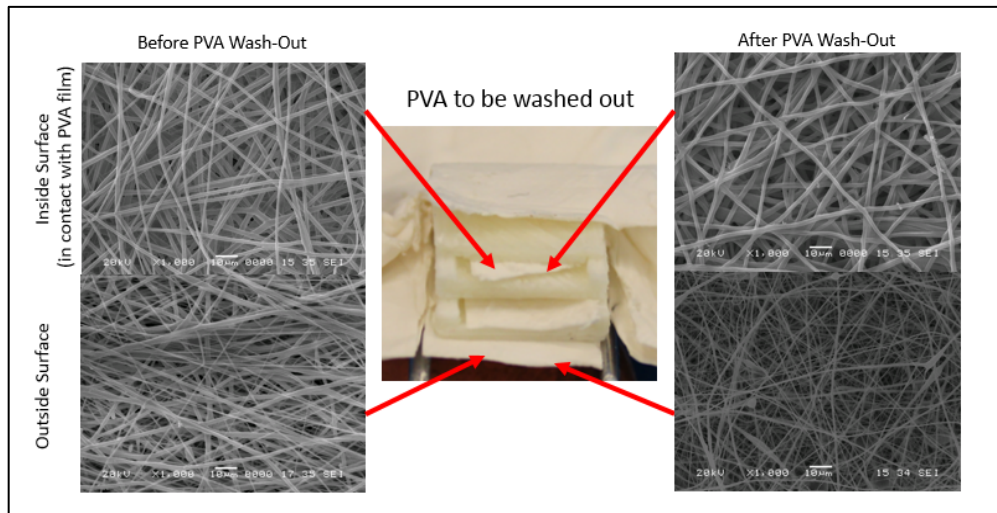


Figure 4: SEM images of fibers before and after PVA wash-out procedure. Center photograph indicates the construct layer that the SEM image was taken from.

2.4 Characterization Methods

2.4.1 Scanning Electron Microscopy

Scanning electron microscopy (SEM, Hitachi SU-70, Tokyo, Japan) was used to obtain low (35-50x) and high magnification (1000x) images of electrospun fibers. Samples were first platinum sputter coated for 85 seconds (Desk V, Denton Vacuum, Moorestown, NJ) to ensure electrical conductivity. Images were obtained at an accelerating voltage of 20 kV, objective aperture of 30 mm, and a working distance of 14 mm. Average fiber diameter and pore size were measured using ImageJ software v1.48 (NIH, Bethesda, MD, USA). Means \pm SD were calculated from three fields of view from each of three samples. Fifty measurements were made for each field of view.

2.4.2 Degradation Characteristics

A degradation timeline for the construct as a whole was determined by placing washed and desiccated samples of known weight in 50 mL of phosphate buffered saline at 37°C on an orbital shaker. Samples were removed from PBS after 0, 60, 84, 108, 132, 176, 200, and 240 hours, rinsed with deionized water, freeze-dried to remove moisture, and reweighed to determine the mass lost. To prevent saturation of solution, PBS was exchanged every other day. The result of the degradation study was calculated as the percentage of mass remaining, using

$$\text{Mass Remaining (\%)} = \frac{M_x}{M_o} \times 100\%$$

where M_o is the initial mass of the construct and M_x is the final weight of the same construct after exposure to the degradation solution for x hours ($n=3$).²⁰

2.4.3 ATR-FTIR

In order to determine if any residues, either from the PVA or the solvent, remained following wash-out of the PVA, or if any alteration in the PGA:PEG bandage had occurred, completed constructs were analyzed by attenuated total reflection Fourier transform infrared (ATR-FTIR) spectroscopy using a Nicolet iS 10 FT-IR spectrometer (ThermoFisher Scientific, Waltham, MA) at a spectral range of 4000-600 cm^{-1} . This measurement evaluated the chemical composition of the electrospun fibers before and after removal of the PVA sacrificial elements to determine if processing altered the materials.²¹⁻²²

2.5 In Vitro Studies

2.5.1 Cell Culture

Human bone marrow derived mesenchymal stem cells (hMSCs, 22 y/o, male, Lonza Biosciences, Walkersville, MD) were used between P4-P6. Cells were cultured in MSC growth media (MSCGM, Lonza Biosciences) in T-75 cell culture flasks at 37°C, 95% relative humidity, and 5% CO₂ with media changes every three days. Cell culture flasks and other reagents were purchased from Fisher Scientific (Hampton, NH) unless otherwise noted.

2.5.2 Biocompatibility Evaluation

We used two approaches to assess the effect of the bandage on a cell payload or on factors produced by those cells and released into the conditioned media. The ability of human MSCs to undergo osteoblast differentiation was used as the model system. In the first set of experiments, we examined the response of MSCs to construct degradation products. In the second set of experiments we examined the osteoblastic differentiation of MSCs cultured on the polymeric scaffold.

2.5.2.1 Effect of construct degradation products

Two constructs were fully degraded in 50 mL growth media to form scaffold-conditioned media (CM). 100µL of an hMSC suspension at a density of 200,000 cells/mL was seeded onto a 12-well tissue culture polystyrene (TCPS) plate with 500µL MSCGM. At 24h, MSCGM was removed, and 500µL of treatment media were added (MSCGM or CM). Media were exchanged every 48h thereafter until harvest at day 5 and at confluence, which occurred on day 7. Culture media were removed and stored at 4°C. The cell layers were rinsed with PBS and frozen with 1mL Triton X-100. Upon thawing, cell layer lysates were homogenized by sonication. DNA content (QuantiFluor, Promega, Madison,

Wisconsin) and alkaline phosphatase specific activity (*p*-nitrophenol released from *p*-nitrophenylphosphate at pH 10.25, normalized to the protein content of lysate) were measured. Conditioned culture media were used to assess release of specific proteins by cells. Enzyme-linked immunosorbent assays (ELISA) were used to quantify vascular endothelial growth factor-A (VEGF¹⁶⁵, R&D Systems, Minneapolis, MN), bone morphogenetic protein 2 (BMP-2, PeproTech, Rocky Hill, New Jersey), osteocalcin (Alfa Aesar, Ward Hill, Massachusetts), and osteoprotegerin (OPG, R&D Systems) following the manufacturer's instructions. Immunoassay results for each culture were normalized to total DNA content.

2.5.2.2 Protein release by MSCs cultured within the PLG:PGA constructs

Each construct used in this set of studies measured 2cm x 2cm and contained a three-layered void. 2.5×10^4 hMSCs suspended in 100 μ L of media were injected into the interior of the construct (via an 18-gauge needle) or seeded onto the surface of a TCPS 12-well plate. Media were exchanged every 48 hours. On day 7, constructs were transferred to new well plates and fresh media were added. Conditioned media were collected 24 hours later (day 8). Cell layers or constructs were rinsed twice with PBS and frozen overnight at -20°C in 1mL of 0.05% Triton X-100 until assayed. Prior to analysis, the lysates were homogenized by sonication and spun in a plate centrifuge to pellet residual polymer to one edge of the plate. DNA content (QuantiFluor, Promega, Madison, Wisconsin) and alkaline phosphatase specific activity were analyzed as above. Conditioned media from the cultures were used to assess protein release by cells. For this study, we measured VEGF, fibroblast growth factor 2 (FGF-2), BMP-2, osteocalcin

and osteoprotegerin by ELISA (R&D Systems, Minneapolis, MN) and data were normalized to total DNA content.

2.5.2.3 Effect of construct on MSC differentiation

25,000 hMSCs were seeded into the construct void space or onto TCPS as previously described. After two days of culture in growth media, one half the cultures were treated with osteogenic media (OM) (Lonza). Media exchanges continued to occur every 48 hours. On day 7, construct samples were transferred to a new plate and with fresh media (either GM or OM). 24 hours later (day 8), media were collected, samples and cell layers were rinsed twice with PBS before being lysed in 1mL of 0.05% Triton X-100. Both media and lysates were frozen overnight and stored at -80°C. Samples were processed as described above.

2.6 Statistical Analysis

The results of quantitative in vitro analyses were calculated as the means \pm SD of six independent cultures per variable. Statistically significant differences between groups were determined by one-way ANOVA followed by Tukey's modification of Student's t-test. p values ≤ 0.05 were considered statistically significant. All in vitro experiments were repeated at least twice to ensure validity of results.

3. Results

3.1 Construct Fabrication and Characterization

In order to identify the best polymer(s) to meet our design criteria, we considered a number of options, including polycaprolactone (PCL), PGA, and PGA:PEG blends. PCL failed to biodegrade over the time course used in the study and was eliminated. Although

PGA monomers are reported to be angiogenic and degradation of the polymer did occur in a time-appropriate manner, we were not able to reliably produce smooth fibers. Addition of PEG as a stabilizer resulted in smooth fibers and analysis of various combinations of PGA and PEG (Figure 2). Based on this study, the best electrospinning parameters were: Solution=140:40 mg/mL PGA:PEG; Flow Rate=2mL/hr; Tip-to-Collector Distance=20cm; Applied Voltage=12.5kV through an 18G blunt-tip needle. An SEM image of the PGA:PEG fibers produced using this method is shown in Figure 2.

3.3 Construct Characterization

3.3.1 Removal of PVA Sacrificial Elements

PVA sacrificial element templates printed at 5x normal size (Figure 3A) dissolved completely after 4 hours (Figure 3B). PVA wash out was confirmed in the final constructs based on SEM micrograph evaluation of samples before and after wash-out (Figure 4). No residue or foreign material could be identified, nor were there any morphological differences between pre- or post-wash fibers.

ATR-FTIR spectra of 'fresh' and 'washed' constructs exhibited matching profiles (Figure 5E), confirming that the process to wash out the PVA sacrificial elements did not chemically change the electrospun fiber material.

3.3.1 Analysis of Fiber Dimensions and Degradation Kinetics

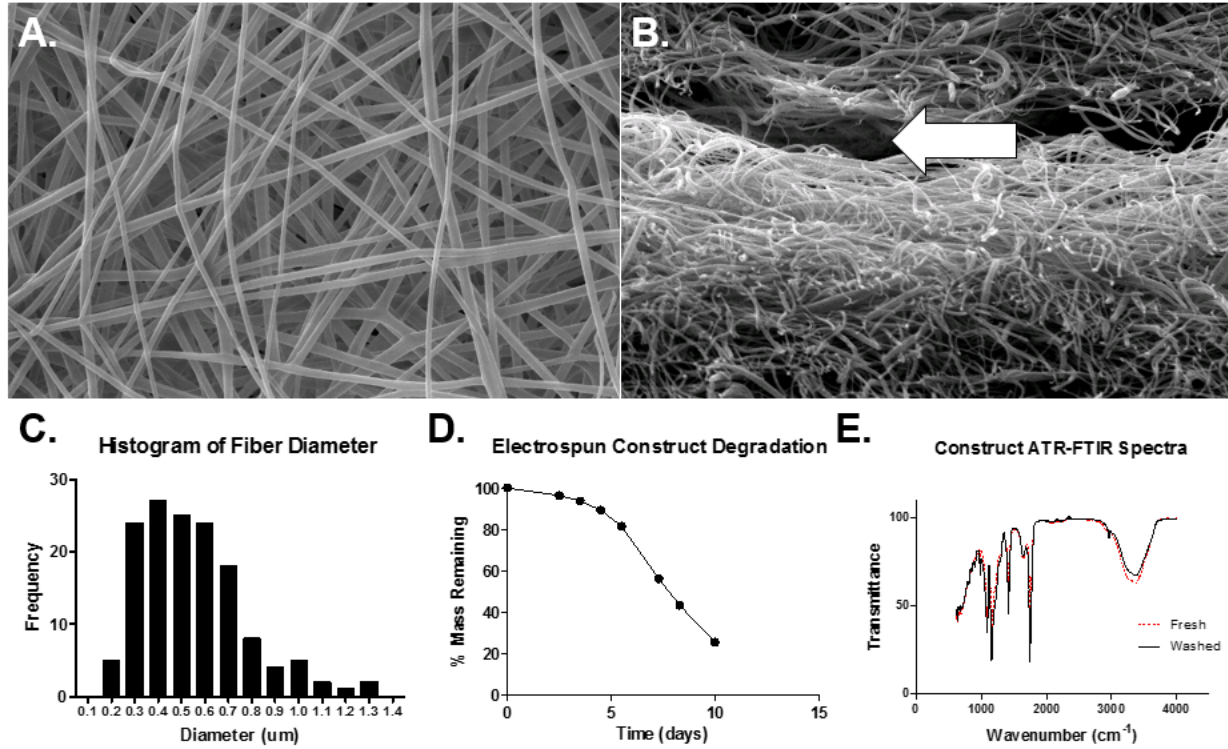


Figure 5: Scanning electron micrographs of electrospun fibers, top view, 1000x (A) and cross-section, 500x (B). Separation of layers created by 3D printed sacrificial elements is noted with white arrow. Distribution of fiber diameters (C), degradation profile (D), and Fourier transform infrared spectra of 'Fresh' and 'Washed' constructs, confirming no chemical alteration due to processing (E).

The non-woven fibrous mesh fabricated by electrospinning resulted in a porous structure of sub-micron diameter fibers. Fibers had a smooth and consistent morphologies (Figure 5A). Cross sections of the mesh showed that fibers were well separated (Figure 5B) and had an average diameter of $0.55\mu\text{m} \pm 0.2\mu\text{m}$ and an average pore size of $3.8\mu\text{m}^2 \pm 2.7\mu\text{m}^2$ (Figure 5C).

When constructs were incubated in aqueous solution, 75% of the electrospun fiber's mass was lost by 10 days (Figure 5D). At this time, constructs lost mechanical stability and began to break apart.

3.4 In Vitro Studies

3.4.1 Biocompatibility

hMSC monolayer cultures that were treated with scaffold degradation byproduct conditioned media (CM) exhibited reduced DNA content (Figure 6A) and alkaline phosphatase specific activity (Figure 6B) compared to cultures treated with growth media (GM). These effects were seen on day 5 and day 7. Production of VEGF was reduced with time, but the type of media had no effect on this parameter (Figure 6C). In contrast, production of BMP-2 was markedly reduced in cultures treated with CM regardless of time (Figure 6D). Osteocalcin production was increased on day 7 in CM treated cultures (Figure 6E) and osteoprotegerin was increased on day 5 in CM cultures (Figure 6F) compared to GM-treated cells.

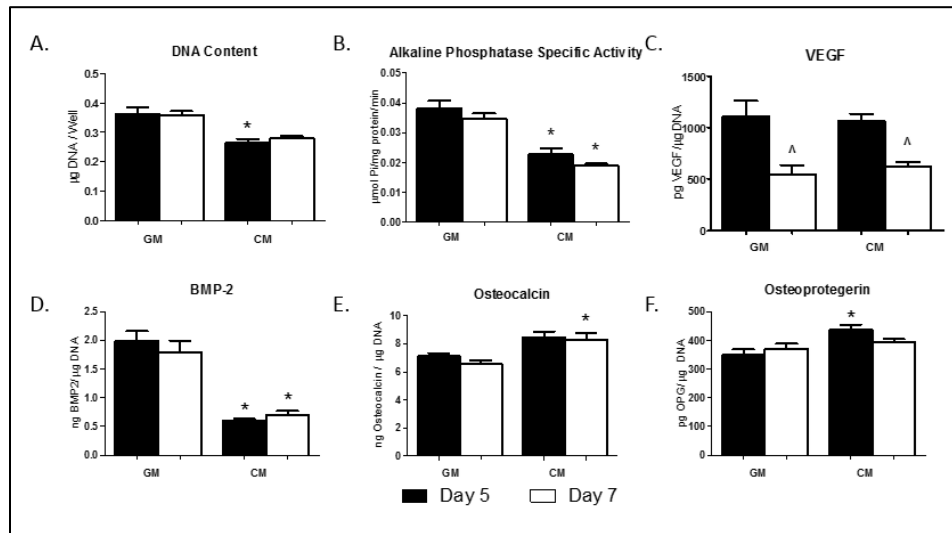


Figure 6: Response of hMSCs cultured with MSCGM media (GM) or construct degradation byproduct conditioned media (CM). DNA content (A) and alkaline phosphatase specific activity (B), with protein quantification by ELISA for VEGF-A (C), BMP-2 (D), osteocalcin (E), and osteoprotegerin (F). Data are from representative experiments and are presented as means \pm SD with n=6 independent cultures, * significant vs GM, $p < 0.05$.

3.4.2 hMSC Response to Growth in the Bandage

Cells that were cultured in growth media within the bandage void space exhibited comparable growth at 8 days as was seen in cultures grown on TCPS (Figure 7A). However, alkaline phosphatase specific activity was markedly higher in the bandage cultures (Figure 7B). Production of growth factors (FGF-2 [Figure 7C], VEGF [Figure 7D] and BMP-2 [Figure 7E]) was comparable under both culture conditions. Similarly, production of osteocalcin (Figure 7F) and osteoprotegerin (Figure 7G) was unaffected by culture conditions.

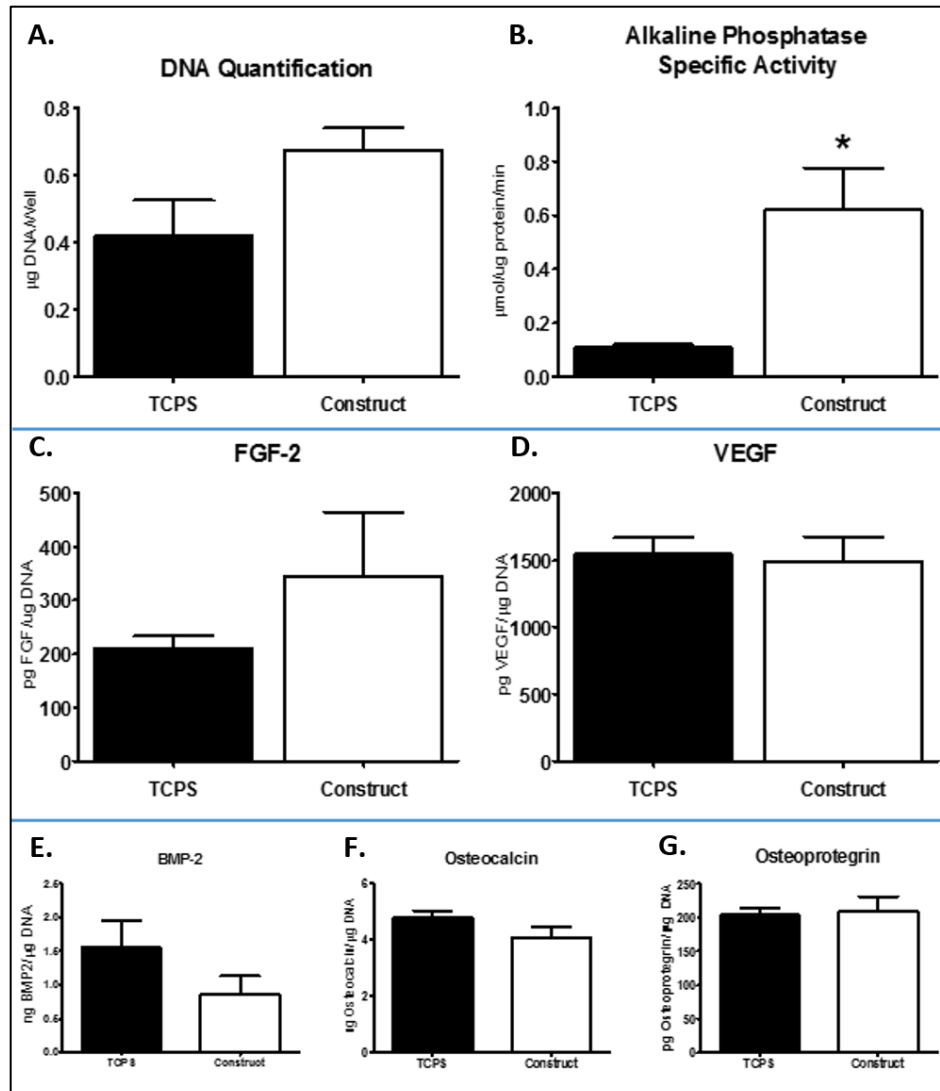


Figure 7: hMSC response to culture within the construct vs. on TCPS. DNA content (A), alkaline phosphatase specific activity (B), FGF-2 (C), and VEGF-A (D). Osteogenic factors were also measured: BMP-2 (E), osteocalcin (F), and osteoprotegrin (G). Data are from one representative experiment and are presented as means \pm SD DNA content per well, alkaline phosphatase specific activity normalized to protein, and specific proteins (C-G) normalized to DNA (n=6 independent cultures; * significant vs TCPS, $p < 0.05$).

3.4.3 hMSC Differentiation within the Bandage

After eight days of growth in either growth media or osteogenic media within the bandage void space, there was no difference in DNA content of cultures (Figure 8A).

Alkaline phosphatase specific activity was significantly reduced in the OM cultures (Figure

8B) whereas production of osteocalcin was significantly increased (Figure 8C). Production of VEGF was comparable under both conditions (Figure 8D), BMP-2 was increased in OM (Figure 8E), and FGF-2 was decreased (Figure 8F).

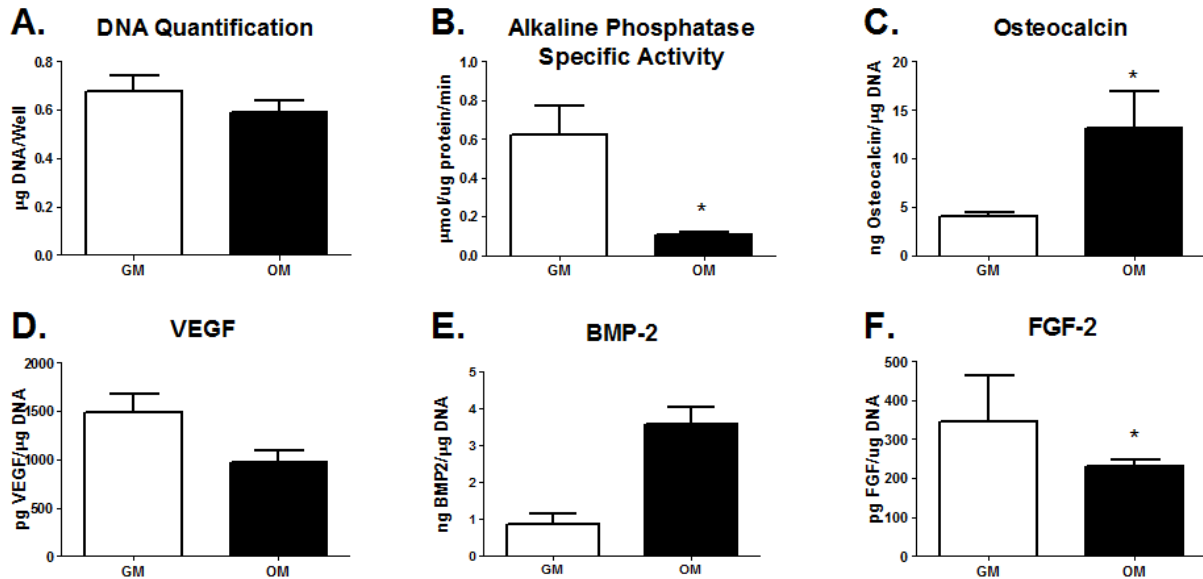


Figure 8: MSCs differentiate within construct in response to osteogenic media. DNA quantification (A), alkaline phosphatase specific activity (B), and levels of osteocalcin (C), VEGF-A (D), BMP-2 (E), and FGF-2 (F). Data are from one representative experiment and are presented as means \pm SD with n=6 independent cultures; * significant vs GM, $p < 0.05$.

4. Discussion

The development of a resorbable dermal wound dressing capable of delivering cells to a wound site holds great potential for a variety of applications. Here, we show that an electrospun construct can be fabricated with an internal reservoir through the use of 3D printed sacrificial elements. The enclosed void space left by the removal of the sacrificial elements provides room for cells to be delivered. It is important that the sacrificial elements are in contact with one another during fabrication to ensure each layer

of the 'reservoir' is interconnected to form a single volume. This method is a significant improvement over other sacrificial element techniques, often using a porogen to manipulate scaffold architecture. This aids the seeding process, allowing a single cell suspension injection to reach all levels of the construct. The presence of electrospun fiber layers through the "reservoir" maximizes the surface area available for cell attachment. The space left by sacrificial elements may also be used to better localize therapeutic agents that are typically delivered as hydrogels or microparticles.²³

Incorporating PEG to the polymer blend not only served as a stabilizer to facilitate electrospinning, but also made the fibers more hydrophilic. Moderate hydrophilicity has been reported to improve protein adsorption and result in better biocompatibility.²⁴⁻²⁸ PEG, which is highly hydrophilic, also reduces the degradation timeframe of the polymer fibers to 10-14 days, which is well coordinated with the documented timeline for full-thickness wound re-epithelialization and angiogenesis. These processes are known to occur around 7 days, or once the granulation tissue has begun to reestablish the wound bed.²⁹ As the construct continues to break down, cells from the surrounding tissue are able to more easily infiltrate the wound site and begin the regeneration and remodeling process. Reestablishment of the absent or damaged tissue is crucial to positive patient outcomes.

In vitro evaluation of the construct has shown it to be supportive of cell growth with minimal influence on cell behavior. Seeding the constructs through suspension injections allows the cells to migrate out through the porous fiber mesh, as opposed to traditional top seeding, which uses gravity to aid cell infiltration. Although the degradation products did have effects on the cells in cultures, it should be noted that cells cultured within the

construct or migrating to the construct would not experience such high levels of degradation byproducts in vivo. Even though media changes reduced exposure to byproducts in vitro, clearance via natural fluid exchange (in vivo) would prevent the accumulation of degradation byproducts on a continuous basis.

Cells remained viable in the constructs over the 8 day culture period with little alteration in growth parameters compared to MSCs grown on TCPS. Only alkaline phosphatase specific activity was elevated. The meaning of this isn't clear. One possibility is that the bandage cells maintained their multipotency, which is ideal in the absence of systemic cues or local factors.³⁰ In contrast, when cells were cultured in OM, alkaline phosphatase was decreased, and osteocalcin production was increased. This suggests the possibility that cells within the constructs were undergoing osteogenic differentiation even in GM and this was accelerated when they were grown in OM. Reduced alkaline phosphatase together with increased osteocalcin is a marker of a well-differentiated osteoblast.³¹ Further support for this is that BMP-2 was also increased in the OM cultures, which potentially contributed to the marked increase in osteocalcin.

5. Conclusion

In this study, a resorbable electrospun wound dressing was prepared that is capable of delivering a payload of cells in effort to enhance defect healing. The PVA sacrificial elements provided an interconnected internal void space and the PGA:PEG blend proved to be degradable along the same 10-14 day timeframe coinciding with normal wound healing. The results indicate that the ability to differentiate is retained by MSCs cultured within the construct and suggest that factors present in the wound site may contribute to the determination of cell fate. This highlights the potential of pre-treating

cells or incorporating factors into the polymer blend to further direct the healing and regeneration process. The combination of 3D printing and electrospun fibers opens possibilities of unique architectures and brings us closer to individualized medicine.

Acknowledgements

This work was funded by a grant from the Department of Defense (W81XWH-11-1-0306).

References

1. O'Meara S, Cullum N, Majid M, Sheldon T. Systematic reviews of wound care management: (3) antimicrobial agents for chronic wounds; (4) diabetic foot ulceration. *Health Technology Assessment*. 2001 May; 4(21):1-237.
2. Kumar P. Classification of skin substitutes. *Burns*. 2008 Feb; 34(1):148-9.
3. Rowan MP, Cancio LC, Elster EA, Burmeister DM, Rose LF, Natesan S, Chan RK, Christy RJ, Chung KK. Burn wound healing and treatment: review and advancements. *Critical Care*. 2015 Jun 12; 19:243.
4. Shores JR, Gabriel A, Gupta S. Skin substitutes and alternatives: a review. *Advanced Skin Wound Care*. 2007 Sep; 20(9 Pt 1): 493-508.
5. Harding KG, Morris HL, Patel GK. Science, medicine and the future: healing chronic wounds. *BMJ*. 2002 Jan 19; 324(7330):16-3.
6. Bonfield W. Designing porous scaffolds for tissue engineering. *Philosophical Transactions. Series A, Mathematical, Physical, and Engineering Sciences*. 2006 Jan 15; 364(1838):227-32.
7. Li WJ, Laurencin CT, Caterson EJ, Tuan RS, Ko FK. Electrospun nanofibrous structure: a novel scaffold for tissue engineering. *Journal of Biomedical Materials Research*. 2002 Jun 15; 60(4):613-21.
8. Drewa T, Galazka P, Prokurat A, Wolski Z, Sir J, Wysocka K, Czajkowski R. Abdominal wall repair using a biodegradable scaffold seeded with cells. *Journal of Pediatric Surgery*. 2005 Feb; 40(2):317-21.

9. Fu Q, Deng CL, Zhao RY, Wang Y, Cao Y. The effect of mechanical extension stimulation combined with epithelial cell sorting on outcomes of implanted tissue-engineered muscular urethras. *Biomaterials*. 2014 Jan; 35(1): 105-12.
10. Boomer L, Liu Y, Mahler N, Johnson J, Zak K, Nelson T, Lannutti J, Besner GE. Scaffolding for challenging environments: materials selection for tissue engineered intestine. *Journal of Biomedical Materials Research A*. 2014 Nov; 102(11):3795-802.
11. Fu K, Pack DW, Kilbanov AM, Langer R. Visual evidence of acidic environment within degrading poly(lactic-co-glycolic acid) (PLGA) microspheres. *Pharmaceutical Research*. 2000 Jan; 17(1): 100-6.
12. Kato Y, Ozawa S, Miyamoto C, Maehata Y, Suzuki A, Maeda T, Baba Y. Acidic extracellular microenvironment and cancer. *Cancer Cell International*. 2013 Sep 3; 13(1):89.
13. Lin HR, Kuo CJ, Yang CY, Shaw SY, Wu YJ. Preparation of macroporous biodegradable PLGA scaffolds for cell attachment with the use of mixed salts as porogen additives. *Journal of Biomedical Materials Research*. 2002; 63(3):271-9.
14. Sadeghi AR, Nokhasteh S, Molavi AM, Khorsand-Ghayeni M, Naderi-Meshkin H, Mahdizadeh A. Surface modification of electrospun PLGA scaffold with collagen for bioengineered skin substitutes. *Material Science and Engineering C Material Biology Applications*. 2016 Sep 1; 66:130-7.
15. Xie SY, Peng LH, Shan YH, Niu J, Xiong J, Gao JQ. Adult Stem Cells Seeded on Electrospinning Silk Fibroin Nanofibrous Scaffold Enhance Wound Repair and

- Regeneration. *Journal of Nanoscience and Nanotechnology*. 2016 Jun; 16(6):5498-505.
16. Liu S, Zhang H, Zhang X, Lu W, Huang X, Xie H, Zhou J, Wang W, Zhang Y, Liu Y, Deng Z, Jin Y. Synergistic angiogenesis promoting effects of extracellular matrix scaffolds and adipose-derived stem cells during wound repair. *Tissue Engineering Part A*. 2011 Mar; 17(5-6):725-39.
17. Eweida AM, Marei MK. Naturally Occurring Extracellular Matrix Scaffolds for Dermal Regeneration: Do They Really Need Cells? *Biomedical Research International*. 2015; 2015:839694.
18. Bonvalle PP, Schultz MJ, Mitchell EH, Bain JL, Culpepper BK, Thomal SJ, Bellis SL. Microporous dermal0mimetic electrospun scaffolds pre-seeded with fibroblasts promote tissue regeneration in full-thickness skin wounds. *Public Library of Science One*. 2015 Mar 20; 10(3):e0122359.
19. Cui W, Zhou Y, Chang J. Electrospun nanofibrous materials for tissue engineering and drug delivery. *Science and Technology of Advanced Materials*. 2010 Mar; 11(1).
20. Okhawilai M, Rangkupan R, Kanokpanont S, DamrongsakkulS. Preparation of Thai silk fibroin/gelatin electrospun fiber mats for controlled release applications. *International Journal of Biological Macromolecules*. 2010 Jun; 46(5):544-50.
21. Chen CH, Lee MY, Shyu VB, Chen YC, Chen CT, Chen JP. Surface modification of polycaprolactone scaffolds fabricated via selective laser sintering for cartilage tissue engineering. *Material Science and Engineering C Materials for Biological Applications*. 2014 Jul 1; 40:389-97.

22. Choudhur M, Mohanty S, Nayak S. Effect of Different Solvents in Solvent Casting of Porous PLA Scaffolds – In Biomedical and Tissue Engineering Applications. *Journal of Biomaterials and Tissue Engineering*. 2015 Jan;5(1).
23. Leslie SK, Cohen DJ, Sedlacek J, Pinsker EJ, Boyan BD, Schwartz Z. Controlled release of rat adipose-derived stem cells from alginate microbeads. *Biomaterials*. 2013 Nov; 34(33):8172-84.
24. Li B, Ma Y, Wang S, Moran PM. A technique for preparing protein gradients on polymeric surfaces: effects on PC12 pheochromocytoma cells. *Biomaterials*. 2005 May; 26(13):1487-95.
25. Kim JH, Kim SH, Kim HK, Akaike T, Kim SC. Adhesion and growth of endothelial cell on amphiphilic PU/PS IPN surface: effect of amphiphilic balance and immobilized collagen. *J Biomedical Materials Research*. 2002 dec 15; 62(4):613-21.
26. Han DK, Park KD, Hubbell JA, Kim YH. Surface characteristics and biocompatibility of lactide-based poly(ethylene glycol) scaffolds for tissue engineering. *Journal of Biomaterials Science Polymer Edition*. 1998; 9(7):667-80.
27. Li B, Ma Y, Wang S, Moran PM. Influence of carboxyl group density on neuron cell attachment and differentiation behavior: gradient-guided neurite outgrowth. *Biomaterials*. 2005 Aug; 26(24):4956-63.
28. Schwartz F, Wieland M, Schwartz Z, Zhao G, Rupp F, Geis-Gerstorfer J, Schedle A, Brogini N, Bornstein MM, Buser D, Ferguson SJ, Becker J, Boyan BD, Cochran DL. Potential of chemically modified hydrophilic surface characteristics

to support tissue integration of titanium dental implants. Journal of Biomedical Materials Research B Applied Biomaterials. 2009 Feb;88(2):544-57.

CHAPTER 3

IN VIVO EVALUATION OF AN ELECTROSPUN AND 3D PRINTED CELLULAR DELIVERY DEVICE FOR DERMAL WOUND HEALING

Authors: Ryan M. Clohessy¹, Karolina Stumbraite¹, David J. Cohen¹, Barbara D. Boyan^{1,2}, Zvi Schwartz^{1,3}

Affiliations: ¹Department of Biomedical Engineering, Virginia Commonwealth University, Richmond, VA, USA; ²Wallace H. Coulter Department of Biomedical Engineering, Georgia Institute of Technology, Atlanta, GA, USA; ³Department of Periodontics, University of Texas Health Science Center at San Antonio, San Antonio, TX, USA

Corresponding Author:

Barbara D. Boyan, Ph.D.

College of Engineering

Virginia Commonwealth University

601 West Main Street

Richmond, Virginia 23284

bboyan@vcu.edu

Running Title: Cell Delivery Device for Dermal Wounds

Keywords: dermal scaffold, electrospinning, 3D printing, wound healing, polyglycolic acid

Abstract

Burns and chronic wounds are especially challenging wounds to heal. In efforts to heal these wounds, physicians often use autologous skin grafts to help restore mechanical and barrier functionality to the wound area. These grafts are, by nature, limited in availability. In an effort to provide an alternative, we have developed an electrospun wound dressing designed to incorporate into the wound with the option to deliver a cellular payload. Here, a blend of polyglycolic acid (PGA) and polyethylene glycol (PEG) was electrospun as part of a custom fabrication method that incorporated 3D printed polyvinyl alcohol (PVA) sacrificial elements. This preparation is unique compared to traditional electrospinning as sacrificial elements provide an internal void space for an injectable payload to be delivered to the wound site. When the construct was tested in vivo (full thickness excisional skin wounds), wound closure was slightly delayed by the presence of the scaffold in both normal and challenged wounds. Quality of healing was improved in normal wounds as measured by histomorphometrics when treated with the construct and exhibited increased neo-vascularization. Stem cell delivery in conjunction with a resorbable extracellular matrix-like scaffold is beneficial to healing of full thickness skin defects and may benefit challenged wounds.

1. Introduction

Large or chronic dermal wounds are unable to restore the barrier that usually protects the body's internal environment without acute medical intervention. The result can reduce the patient's quality of life and lead to loss of limb or life. Each year approximately 5.7 million patients seek treatment for dermal wounds in the U.S. alone, costing an estimated \$25 billion. In addition to this, nearly 500,000 patients seek treatment for burn and other injuries requiring skin grafts [1]. Current treatments for dermal wounds include autografts, allografts, xenografts and more recently synthetic dressings or skin substitutes. Autografts, the gold standard for skin grafts, minimize the possibility of rejection or disease transmission through their inherent nature of being the native tissue [2]. This procedure leaves a painful secondary wound site and processing the skin undergoes before application often leads to extensive scarring [3].

Tissue engineering approaches to treating dermal wounds have gained popularity in the recent years. Acellular grafts, made of collagen, hyaluronic acid, or decellularized matrices are becoming more popular [4-6]. Synthetic cellular grafts made of biodegradable films cultured with autologous, allogeneic or recombinant skin cells have begun to be made commercially available [7]. Although the use of engineered grafts is a step forward in wound healing technology, they experience some of the drawbacks of conventional skin grafts, such as a high risk of rejection, transmission of infection, excess scarring, and expense to the patient and care providers [3]. Therefore, there is a great need for a synthetic, off-the-shelf wound dressing that can be integrated to the tissue as a graft.

Electrospinning, a versatile process that can produce micro- to nano-sized fibers from a polymeric solution, can closely mimic the extracellular matrix [8, 9]. We applied this technique to produce a randomly oriented microfiber scaffold from two polymers, poly(glycolic acid) (PGA) and poly(ethylene glycol) (PEG), with an addition of a void space pocket to allow for a payload of cells or therapeutic agents. PGA is a biodegradable polymer that is found most commonly in absorbable surgical sutures. PGA has been shown to support a variety of cells [10-12] and can also result in an acidic microenvironment at the wound site [13], which has been shown to have pro-angiogenic influences [14]. PEG is a water-soluble polymer that serves to aid in the electrospinning process and increase the degradation rate. The combination of these two FDA approved polymers facilitates more uniform electrospun fibers, as well as allowing modification of the degradation timeframe [15]. The randomly oriented fibers of the scaffold allow native cells from the wound site to attach and begin their healing and remodeling processes [16].

By incorporating an internal void space, a payload can be delivered to the wound site. The addition of encapsulated mesenchymal stem cells (MSCs) and adipose derived stem cells (ASCs) to wound sites has been noted to improve healing and regeneration outcomes, in part by stimulating angiogenesis via the production of angiogenic factors [17-21]. However, many of the approaches used to deliver MSCs have size constraints affecting diffusion of nutrients and waste products. Using 3D printing, nearly limitless configurations of the cargo area can be designed and included within the construct. Here we chose a 1cm x 1cm square template as this resulted in a construct that nicely fit the selected wound model.

The aim of this study was to evaluate the in vivo effectiveness of a resorbable dermal wound dressing that could deliver and localize a payload of cells while serving as a matrix for host cell ingrowth. Previous in vitro studies in our lab showed that human MSCs cultured in this scaffold remained viable over time and produced factors that were secreted into the surrounding media. Moreover, the cells responded to exogenous factors, indicating that their ability to differentiate was not impeded by the polymer scaffold (Clohessy et al. Development of a biodegradable three-dimensional cell delivery bandage. Mater Sci Eng C Mater Biol Appl. Under Review). Based on these in vitro observations, the construct was hypothesized to support tissue regeneration and aid in the wound healing process with pre-seeded constructs further improving healing in full-thickness dermal wounds. To test this hypothesis, we applied both seeded and unseeded constructs to full thickness excisional wounds. The effects on wound closure, tissue regeneration, and angiogenesis were investigated using both normal and ischemic wound models.

2. Materials and methods

2.1 Construct fabrication

Electrospun constructs were fabricated using a combination of techniques, as described previously (Clohessy et al. Development of a biodegradable three-dimensional cell delivery bandage. Mater Sci Eng C Mater Biol Appl. Under Review). Sub-micron fibers were vertically electrospun using a solution of 140 mg/mL polyglycolic acid (PGA, i.v. 1.0-2.0, Polysciences Inc., Warrington, PA) and 40 mg/mL polyethylene glycol (PEG, Mw=20,000, Sigma Aldrich, St. Louis, MO) in 1,1,1,3,3,3-hexafluoro-2-propanol (HFIP, Sigma Aldrich). The polymer was extruded through a blunt-tipped 18-gauge needle at

2mL/h with an applied voltage of 12.5 kV onto a flat aluminum foil target at a 30cm collection distance. Layers of electrospun fibers were alternated with 3D printed void templates until the seven-layer construct was complete. Before positioning the second and third layers of 3D printed sacrificial elements, small cuts were made in the covering electrospun fiber layer to allow contact between sacrificial elements along two parallel edges. These cuts allowed the sacrificial elements to form one interconnected “reservoir.” The 1cm x 1cm x 0.08cm 3D printed sacrificial elements were printed from 1.75mm diameter polyvinyl alcohol filament (Ultimachine, South Pittsburgh, TN) on a MakerBot Replicator 2X (MakerBot, New York, NY) and designed for interconnection. The completed “fresh” constructs were then soaked in deionized water (DI-H₂O) for 24 h to remove the PVA void templates, leaving an interconnected void within the electrospun fibers of the “washed” construct. A schematic of the process can be seen in Figure 1A. Sterilization of the construct was accomplished by soaking in 70% ethanol for 1 h followed by three five-minute rinses in sterile PBS under aseptic technique.

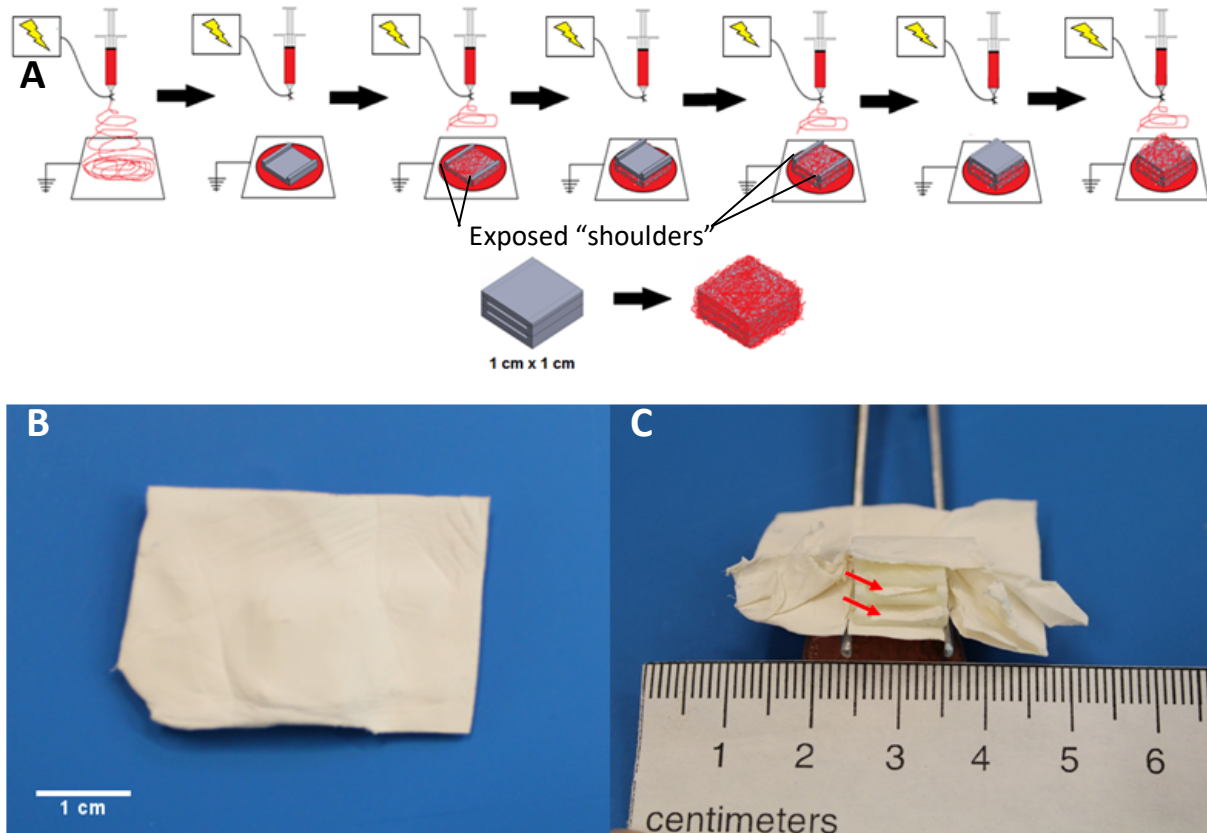


Figure 1: Schematic of fabrication process (A). Photograph of construct as-fabricated (B), and bisected to reveal internal composition (C).

2.2 In vivo model

Both normal and compromised (ischemic) full-thickness wounds were used to evaluate the effects of the construct. All experiments were conducted under an approved Institutional Animal Care and Use protocol at Virginia Commonwealth University. Skeletally mature, male Sprague Dawley rats weighing $400 \pm 25\text{g}$ were obtained from Harlan Laboratories (Indianapolis, IN). Rats were given full anesthesia through flowing isoflurane (1.5% in 1 L/min O₂); afterward, the hair over the dorsum was clipped and the skin was scrubbed with 70% ethanol solution and chlorhexidine to prepare for wounding. Subcutaneous injections of extended release analgesic, buprenorphine XR, were

administered at 1.2mg/kg body weight immediately preceding surgery. The center of each wound was marked 1.5cm below the scapula and 1.0cm to either side of the spine. Prior to wound creation, silicone doughnuts 2cm in diameter with 1.5cm inner diameter and thickness of 1.7mm (GBL665283, Grace Bio-Labs, Bend, OR) were fixed around the wound site using surgical glue (Henry Schein, Melville, NY) and sutured in place (Look 5-0 Black Mono Nylon Sutures, Ace Surgical, Brockton, MA). Within each doughnut, a 10mm full-thickness wound was made with a sterile biopsy punch (NC9226137, Fisher Scientific, Hampton, NH). The doughnuts were used to prevent wound contraction and allow the wound to heal by secondary intention in an effort to make the model more analogous to human wound healing [22-24]. Wound contraction in rat models is a well-documented phenomenon, yet is predominantly ignored throughout the literature [25-27].

An ischemic model was used to model compromised wound healing [28]. In this model, both splinted wounds were within a 4.25cm by 3cm, cranially oriented, $\frac{3}{4}$ pedicle flap that was separated from the underlying fascia with a 4cm x 3cm x 0.5mm silicone isolator sheet (GBL665283, Grace Bio-Labs, Bend, OR). Isolators were sutured in place with undyed 5-0 PGA sutures (PSN421V, Hu-Friedy, Chicago, IL).

All constructs were sutured in place with PGA sutures and wounds were covered in a clear wound dressing (Tegaderm, 3M Health Care, St. Paul, MN), padded with steam sterilized gauze and wrapped in elastic fabric tape. Upon recovery from anesthesia, animals were returned to their singly housed home cage. Surgeries were conducted in a random order with respect to model, treatment group. At the end of the study, animals were euthanized by CO₂ asphyxiation. All in vivo experiments were approved by VCU Institutional Animal Care and Use Committee (IACUC).

2.2.1 Animal study #1

The first in vivo study was designed to evaluate the effects the construct alone may have on wound healing while ensuring no adverse effects resulting from implantation. 32 rats underwent the surgical procedure described above. One wound in each animal was treated with an electrospun construct, while the other was left untreated as a control. Animals were imaged every other day and allowed to heal for 10 or 21 days. Eight wounds were examined for each group (Empty or Construct) in each of the normal and ischemic models at each time point. Wounds and surrounding tissue were harvested for histology, qualitative grading, and quantitative histomorphometric measurements.

2.2.2 Animal study #2

A second study was designed to evaluate the constructs pre-seeded with stem cells. Sprague Dawley rat ASCs were selected to avoid the possibility of xenogenic rejection. ASCs that had been isolated from the inguinal fat pads of male Sprague Dawley rats were used between P4-P6. Cells were cultured in T-75 cell culture flasks at 37°C, 95% relative humidity, and 5% CO₂ with MSCGM basal media (Lonza, Basel, Switzerland) changes every three days. Cell culture components and other reagents were purchased from Fisher Scientific (Hampton, NH) unless otherwise noted. Prepared constructs were seeded with 50,000 ASCs 48 hours before implantation and cultured in MSCGM supplemented with 10% Sprague Dawley rat serum (Innovative Research, Novi, MI).

Both the normal and ischemic models were used with treatment groups consisting of: empty (negative control), unseeded construct, or seeded construct. 24 animals

underwent the procedure described above with four animals in each group. Both wounds in each animal received the same treatment group in order to prevent implanted cell migration or construct degradation byproducts from affecting the contralateral wound. Animals were imaged every other day and allowed to heal for 21 days. In this study, only one timepoint was selected to evaluate the wounds once the constructs had degraded. Wounds and surrounding tissue were harvested for histology, qualitative grading, quantitative histomorphometric measurements and immunohistochemistry. Eight wounds were examined for each group (Empty, Unseeded, Seeded) in each of the normal and ischemic models.

2.3 Wound closure analysis

Dermal wounds were imaged every other day. Wound area was quantified by tracing the wound border in each photograph (ImageJ v1.48, NIH, Bethesda, MD). The scale was set to a ruler photographed with each wound and wound percentage was calculated as follows:

$$\text{Relative Wound Area} = \frac{\text{Area on day}(n)}{\text{Area on day}(1)}$$

2.3.1 Histology

Wounds and surrounding tissue (2cm x 2cm) were resected and fixed overnight in 10% neutral buffered formalin. Samples were processed (STP 120, Thermo Fisher Scientific, Waltham, MA) and embedded in paraffin. Histological sections (5µm thickness) were stained with H&E. Slides were imaged using transmitted light bright field microscope (Zeiss Observer Z1, Oberkochen, Germany) equipped with a 2.5x objective and 10x

optical zoom. Images were captured by an AxioCam MRc5 camera with Zeiss ZEN Pro Blue Edition software (Oberkochen, Germany).

2.3.2 Quantitative histomorphometrics

From images of the H&E stained sections, quantitative histomorphometrics were performed measuring the abnormal tissue length, distance un-epithelialized, and wound thickness ratio using criteria adapted from adapted from Lemo et al. 2010. Abnormal tissue length represents the distance of the wound that has not been remodeled. Un-epithelialized distance represents the length of tissue not epithelialized or a gap in the tissue. The wound thickness ratio represents the average thickness of the visible wound area relative to the average thickness of the healthy tissue along the margins of the wound.

2.3.4 Qualitative histological grading

H&E stained sections were blindly graded by three trained graders. Grading criteria was adapted from Altavilla et al. [29]; Sections were scored on a scale of 0-4 in epidermal regeneration, dermal regeneration and granulation tissue thickness (see Table 1).

2.3.4 Immunohistochemistry

To evaluate the effect of constructs on angiogenesis, sections were fluorescently stained for alpha smooth muscle actin to identify blood vessels [30]. Antigen retrieval was performed on deparaffinized samples in 1mM EDTA at pH 8.0 at 95°C for 5min, and then cooled to room temperature. Samples were then rinsed and blocked with StartingBlock (PI37538, Thermo Fisher Scientific). Anti-alpha smooth muscle actin primary antibody (ab5694, abcam, Cambridge, UK) was applied overnight at a 1:250 dilution in PBS, 0.05%

Tween 20. The secondary antibody, Goat anti-mouse IgG Alexa Fluor 488 (Invitrogen, A11001) secondary antibody was applied for two hours at 1:200 dilution in PBS, 0.05% Tween 20, 1% BSA and counterstained with pentahydrate (bis-benzimide) for 20 minutes (Hoechst 33258, Molecular Probes, Eugene, OR). Slides were then imaged using fluorescent light on a Zeiss Observer Z1 microscope equipped with a 2.5x objective and 10x optical zoom. Images were captured by an AxioCam MRc5 camera and images were compiled using Zeiss ZEN Pro Blue Edition software.

2.4 Statistical analysis

Experiment analyses were calculated as the means \pm SEM of eight samples per variable. Statistically significant differences between groups were determined by one-way ANOVA followed by Tukey's modification of Student's t-test. p values ≤ 0.05 were considered statistically significant.

3. Results

3.1 Construct fabrication

The appearance of an 'as-fabricated' construct can be seen in Figure 1B with an exploded view (Figure 1C) highlighting the internal, interconnected PVA sacrificial elements interpolated with electrospun fibers (red arrows). PVA was found to fully dissolve in static H₂O within 4 hours, and when enveloped in electrospun fibers, within 24 hours. All samples underwent 24 hours of PVA washout before disinfection and use in described studies.

3.2 In vivo study #1

Electrospun constructs had no adverse effects on the animals' overall health or wellbeing over the course of the study. In normal wounds, closure was slightly delayed by the construct at day 10, but quickly recovered to the empty control (Fig. 2A).

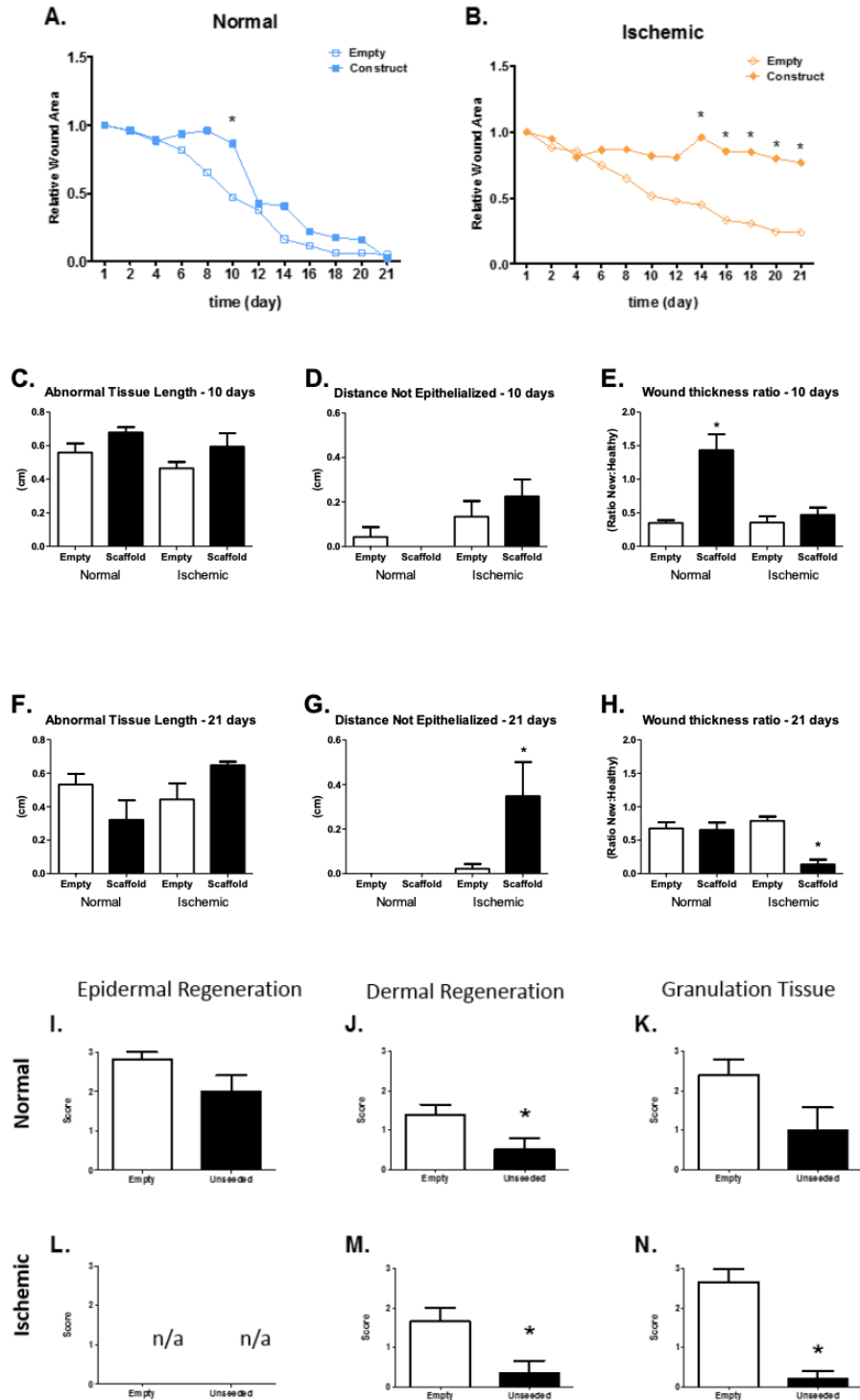


Figure 2: In vivo study #1 results with wounds treated with unseeded constructs or left empty. Wound closure data for normal (A) and ischemic (B) wounds over time. Histomorphometrics for normal wounds (C-E) and ischemic wounds (F-H). Scores from H&E grading for normal wounds (I-K) and ischemic wounds (L-N).

However, in the ischemic wounds there was greater divergence between the empty and construct treated wounds, with days 14-21 having significantly larger wound areas (Fig. 2B). The construct treated ischemic wounds did not successfully heal and maintained a wound area nearly 80% of the original for the duration of the study.

Representative images of H&E staining of histological sections for the four groups (normal empty, normal construct treated, ischemic empty, ischemic construct treated) can be seen in Figure 3. At 10 days, the scaffold treated normal wounds measured thicker relative new tissue depth compared to all other groups (Fig. 2E).

At 21 days, the construct treated ischemic group had a significantly thinner new tissue depth and a higher incidence of remaining unepithelialized area (Fig. 2, F-G). The scaffold treated normal group had re-epithelialization in all samples (Fig. 2 D, G).

Scoring of the wounds (Fig. 2, C-N) revealed lower dermal regeneration of the construct treated wounds in both the normal and ischemic groups. The construct was also found to have a lower score in the granulation tissue thickness category for the ischemic model.

Fluorescent staining for α -SMA, indicated blood vessels within the regenerating tissue. Construct treated normal wounds had significantly higher number of blood vessels per field of view, roughly three times higher than wounds left empty. The ischemic wounds lacked significance, but also maintained a higher average than the empty groups.

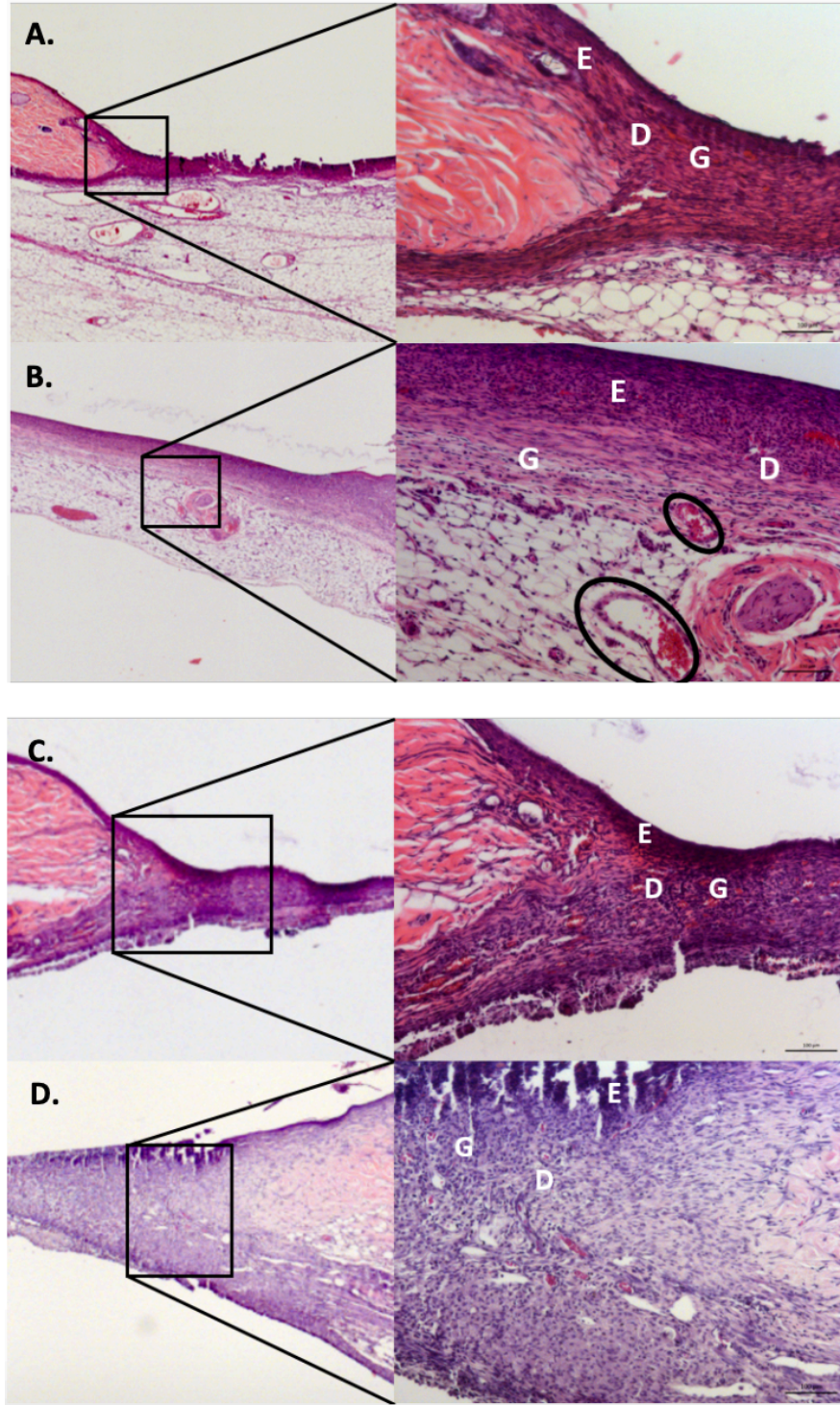


Figure 3: Representative H&E stained slides for normal empty (A), normal construct treated (B), ischemic empty (C), and ischemic construct treated (D) at 2.5x in the left column. Pop-outs are 10x regions of interest with granulation tissue, dermal regeneration, and epidermal regeneration labeled with white letters G, D, and E respectively.

3.3 In vivo study #2

The relative wound area for either seeded or unseeded construct treated wounds in the normal animals was significantly different from the empty treatment at days nine and 11, with the unseeded group continuing to be different from the empty treatment through day 13 (Fig. 4, A-B). In the ischemic animals the findings were statistically indifferent to the treatment group. The normal animals were able to completely close the wounds while the ischemic animals maintained a wound area at the end of the study. It was noted that the wound splints began to fail at day 15, which could lead to inaccurate wound closure measurements. Due to this, the data presented are for the days that the splints remained intact (d0-d15).

Histological morphometric measurements (Fig. 4, C-H) and scoring (Fig. 4, I-N) failed to find many significant differences, the only being the unseeded construct-treated normal wound had less dermal regeneration than the empty normal wound. Representative images of H&E stained sections can be seen in Figure 5.

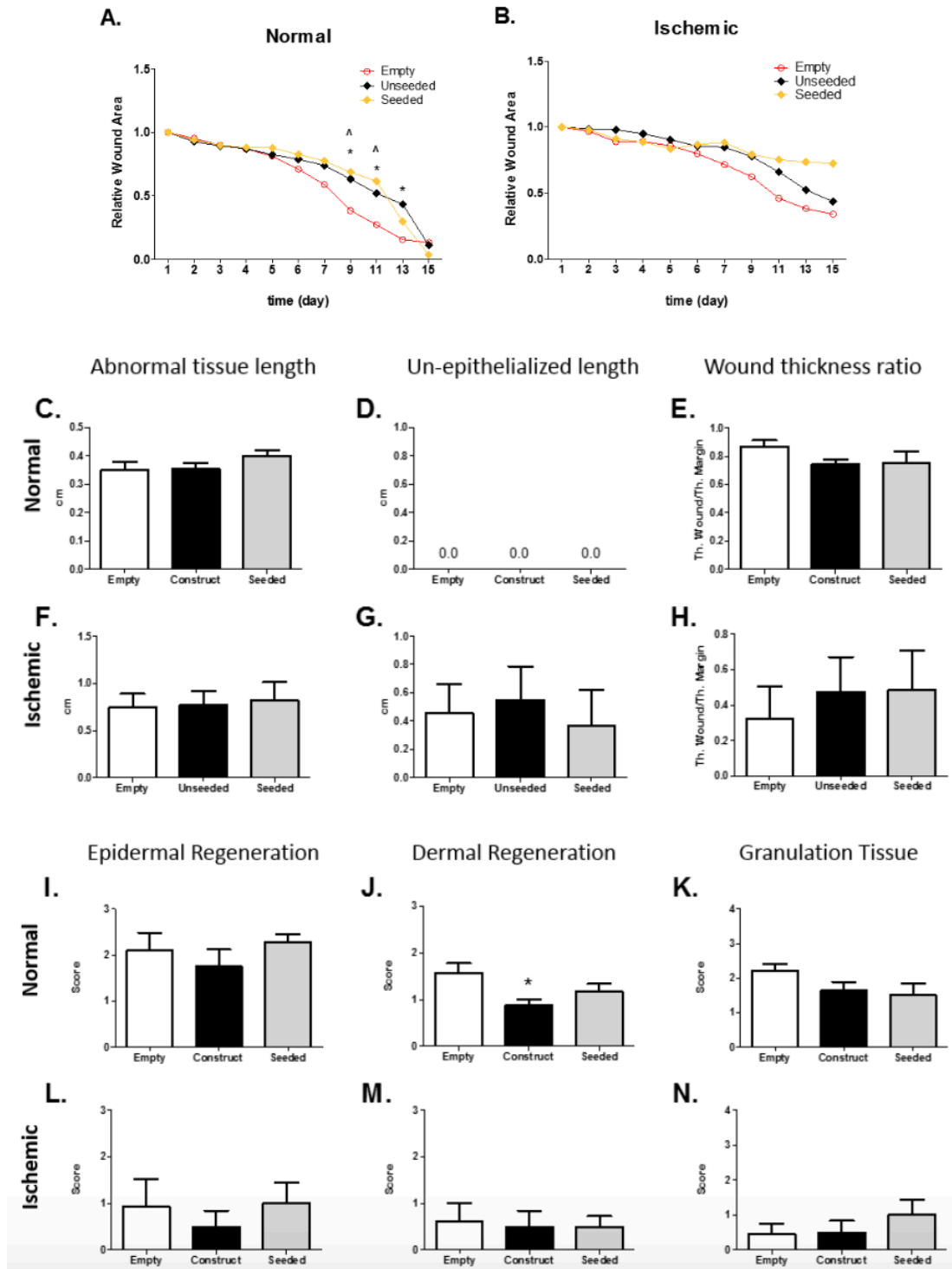


Figure 4: In vivo study #2 results with wounds treated with seeded constructs, unseeded constructs or left empty. Wound closure data for normal (A) and ischemic (B) wounds over time. Histomorphometrics for normal wounds (C-E) and ischemic wounds (F-H). Scores from H&E grading for normal wounds (I-K) and ischemic wounds (L-N).

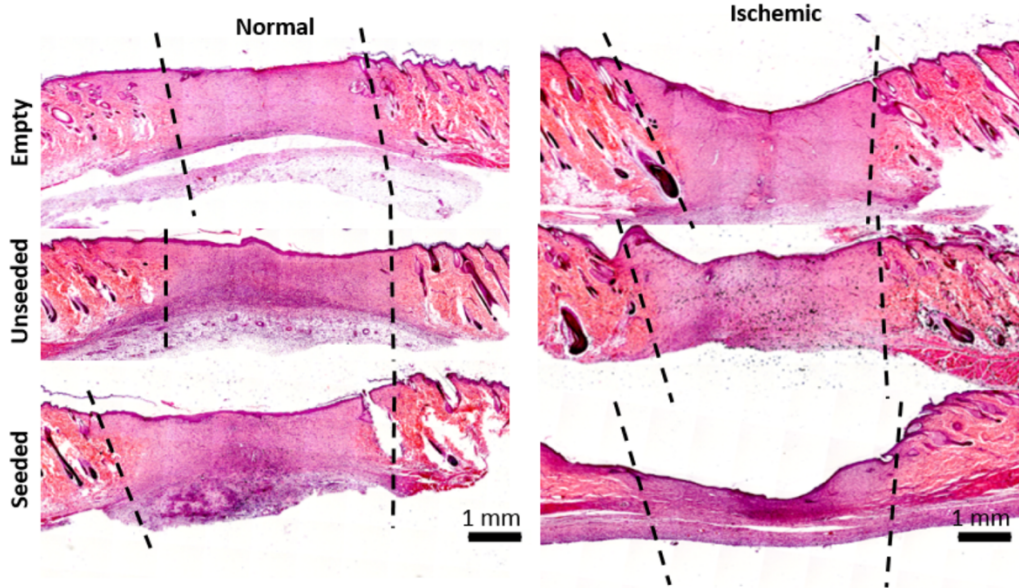


Figure 5: Representative images of 2.5x H&E stained sections with normal wounds (left) and ischemic wounds (right) and left empty (first row), treated with an unseeded construct (second row) or a ratASC seeded construct (third row). Wound margins are noted with dashed line.

Immunohistochemical staining of α -smooth muscle actin was again able to identify a nearly three-fold increase in blood vessels found within sections of normal wounds treated with either seeded or unseeded constructs (Fig. 6, A-B). Differences were not found among the ischemic wounds.

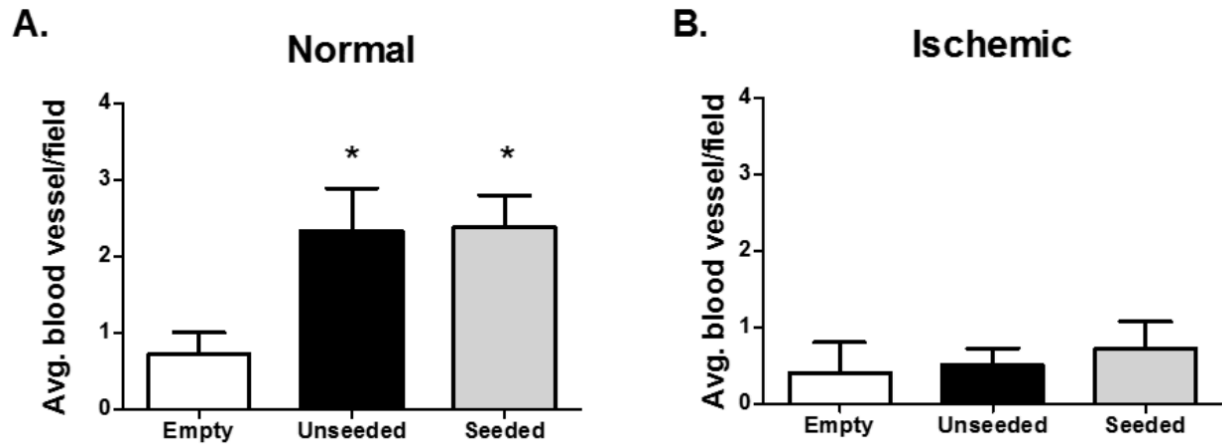


Figure 6: Average blood vessel counts per field of view for normal (A) and ischemic (B) wounds. Empty and unseeded groups are from both in vivo studies.

4. Discussion

The development of a resorbable dermal wound dressing capable of delivering cells to a wound site holds great potential. Here, we show that an electrospun construct can be fabricated with an internal reservoir through the use of 3D printed sacrificial elements. The enclosed void space left by the removal of the sacrificial elements provides room for cells to be delivered. It is important that the sacrificial elements are in contact with one another during fabrication to ensure each layer of the ‘reservoir’ is interconnected to form single volume. This method is a significant improvement over other sacrificial element techniques often using a porogen to manipulate scaffold architecture. This aids the seeding process, allowing a single cell suspension injection to reach all levels of the construct. The presence of electrospun fiber layers through the “reservoir” maximizes the surface area available for cell attachment. The space left by sacrificial elements may also be used to better localize therapeutic agents that are typically delivered as hydrogels or microparticles [31].

In these studies, we see the normal wounds were able to develop more granulation tissue in the wound site than the ischemic wounds. This is due to the basement of the wound being able (normal wounds) or unable (ischemic wounds) to participate in replenishing the defect. Re-epithelialization of the wounds was found to be faster in the construct treated groups suggesting that at earlier times, the scaffold may act as a substrate for the native keratinocytes to repopulate the wound area. The increase in blood vessels found in both studies is believed to be a result of the construct degrading and creating an acidic microenvironment. Low microenvironmental pH is known to be pro-angiogenic through the induction of vascular endothelial growth factor (VEGF) via the hypoxia-inducible transcription factor (HIF)-1 pathway [14]. The increase in neo-vascularization supports the construct is able to aid wound healing.

This study has also found delays in wound closure rates for samples treated with the constructs. Although the constructs are shown to support cell attachment, re-epithelialization, and increased angiogenesis, they may also act as a physical barrier to the proliferation and remodeling by native cells. This was found to persist until approximately day 10 when the construct had degraded enough to allow for complete infiltration and wound closure. The ischemic wounds lacked the clearance to efficiently degrade the scaffold, which visibly remained through 21 days. A result of the ischemic isolator, the limited perfusion and low volume of healthy tissue in contact with the wound site was severely limiting in regenerative ability and has proven an extremely challenging model to successfully heal. The lack of differences between the seeded construct and the unseeded or empty control among the histomorphometrics and wound closure rates was

surprising considering the beneficial effect exogenous MSCs have on wound healing, namely their ability to recruit other host cells and secrete growth factors [32].

Conclusion

In this study, a resorbable electrospun wound dressing was prepared that was capable of delivering a payload of cells in effort to enhance the healing of dermal defects. Delivered cells maintained their behavior in vitro, but at this stage were ineffective in accelerating wound healing in vivo. Despite marginal healing in vivo, the construct could easily be used as a delivery device for a variety of therapeutics such as an analgesic, an anti-microbial or anti-scarring agent. Results confirm the construct can serve as a substrate for re-epithelialization and increase blood vessel formation in the normal wound model. This increase in vascularity over the untreated wounds is significant as vascularization is paramount to healing potential. The ischemic model was successfully implemented as a compromised wound model but proved exceptionally challenging to heal. This study is also believed to be the first where both wound splints and an ischemic model were used simultaneously. Although the construct did not augment wound closure at this stage, the technology remains a promising option for a resorbable, therapeutic delivering wound dressing. It is also important to note that the speed of healing is directly related to the quality of regenerated tissue, with very rapid wound closure often leading to extensive scarring, thus the delayed wound closure found in construct treated wounds may not be explicitly detrimental. Evaluating the wound closure at a later time would allow the evaluation of the regenerated skin quality opposed to wound size and histological analysis conducted here. Improving construct integration as well as potentially adding exogenous factors to push differentiation, pretreating loaded cells, or seeding multiple

types of cells may also improve the efficacy of the wound dressing and must be further investigated the construct's full potential in multiple applications

Acknowledgements

This research was funded through a grant from the US Department of Defense (W81XWH-11-1-0306).

References

1. Sen CK, Gordillo GM, Roy S, Kirsner R, Lambert L, Hunt TK, Gottrup F, Gurtner GC, Longaker MT. Human Skin Wounds: A Major and Snowballing Threat to Public Health and the Economy. *Wound Repair Regen.* 2009 Nov-Dec; 17(6): 763-771.
2. Smith OJ, Edmondson SJ, Bystrzonowski N, Hachach-Haram N, Kanapathy M, Richards T, Mosahebi A. The CelluTome epidermal graft-harvesting system: a patient-reported outcome measure and cost evaluation study. *Int Wound J.* 2016 Aug 4. [Epub]
3. Harding KG, Morris HL, Patel GK. Science, medicine and the future: healing chronic wounds. *BMJ.* 2002 Jan 19; 324(7330):16-3.
4. O'Meara S, Cullum N, Majid M, Sheldon T. Systematic reviews of wound care management: (3) antimicrobial agents for chronic wounds; (4) diabetic foot ulceration. *Health Technol Assess.* 2000; 4(21):1-237.
5. Kumar P. Classification of skin substitutes. *Burns.* 2008 Feb; 34(1):148-9.
6. Rowan MP, Cancio LC, Elster EA, Burmeister DM, Rose LF, Natesan S, Chan RK, Christy RJ, Chung KK. Burn wound healing and treatment: review and advancements. *Crit Care.* 2015 Jun 12; 19:243.
7. Shores JR, Gabriel A, Gupta S. Skin substitutes and alternatives: a review. *Adv Skin Wound Care.* 2007 Sep; 20(9 Pt 1): 493-508.
8. Bonfield W. Designing porous scaffolds for tissue engineering. *Philos Trans A Math Phys Eng Sci.* 2006 Jan 15; 364(1838):227-32.

9. Li WJ, Laurencin CT, Caterson EJ, Tuan RS, Ko FK. Electrospun nanofibrous structure: a novel scaffold for tissue engineering. *J Biomed Mater Res.* 2002 Jun 15; 60(4):613-21.
10. Drewa T, Galazka P, Prokurat A, Wolski Z, Sir J, Wysocka K, Czajkowski R. Abdominal wall repair using a biodegradable scaffold seeded with cells. *J Pediatr Surg.* 2005 Feb; 40(2):317-21.
11. Fu Q, Deng CL, Zhao RY, Wang Y, Cao Y. The effect of mechanical extension stimulation combined with epithelial cell sorting on outcomes of implanted tissue-engineered muscular urethras. *Biomaterials.* 2014 Jan; 35(1): 105-12.
12. Boomer L, Liu Y, Mahler N, Johnson J, Zak K, Nelson T, Lannutti J, Besner GE. Scaffolding for challenging environments: materials selection for tissue engineered intestine. *J Biomed Mater Res A.* 2014 Nov; 102(11):3795-802.
13. Fu K, Pack DW, Kilbanov AM, Langer R. Visual evidence of acidic environment within degrading poly(lactic-co-glycolic acid) (PLGA) microspheres. *Pharm Res.* 2000 Jan; 17(1): 100-6.
14. Kato Y, Ozawa S, Miyamoto C, Maehata Y, Suzuki A, Maeda T, Baba Y. Acidic extracellular microenvironment and cancer. *Cancer Cell Int.* 2013 Sep 3; 13(1):89.
15. Lin HR, Kuo CJ, Yang CY, Shaw SY, Wu YJ. Preparation of macroporous biodegradable PLGA scaffolds for cell attachment with the use of mixed salts as porogen additives. *J Biomed Mater Res.* 2002; 63(3):271-9.
16. Sadeghi AR, Nokhasteh S, Molavi AM, Khorsand-Ghayeni M, Naderi-Meshkin H, Mahdizadeh A. Surface modification of electrospun PLGA scaffold with collagen

- for bioengineered skin substitutes. *Mater Sci Eng C Mater Biol Appl.* 2016 Sep 1; 66:130-7.
17. Lee CS, Burns OA, Raghuram V, Kalisvaart J, Boyan BD, Schwartz Z. Adipose stem cells can secrete angiogenic factors that inhibit hyaline cartilage regeneration. *Stem Cell Res Ther.* 2012 Aug 24;3(4):35.
18. Xie SY, Peng LH, Shan YH, Niu J, Xiong J, Gao JQ. Adult Stem Cells Seeded on Electrospinning Silk Fibroin Nanofibrous Scaffold Enhance Wound Repair and Regeneration. *J Nanosci Nanotechnol.* 2016 Jun; 16(6):5498-505.
19. Liu S, Zhang H, Zhang X, Lu W, Huang X, Xie H, Zhou J, Wang W, Zhang Y, Liu Y, Deng Z, Jin Y. Synergistic angiogenesis promoting effects of extracellular matrix scaffolds and adipose-derived stem cells during wound repair. *Tissue Eng Part A.* 2011 Mar; 17(5-6):725-39.
20. Eweida AM, Marei MK. Naturally Occurring Extracellular Matrix Scaffolds for Dermal Regeneration: Do They Really Need Cells? *Biomed Res Int.* 2015; 2015:839694.
21. Bonvalle PP, Schultz MJ, Mitchell EH, Bain JL, Culpepper BK, Thomal SJ, Bellis SL. Microporous dermal mimetic electrospun scaffolds pre-seeded with fibroblasts promote tissue regeneration in full-thickness skin wounds. *PLoS One.* 2015 Mar 20; 10(3):e0122359.
22. Scharstuhl A, Mutsaers HA, Pennings SW, Szark WA, Russel FG, Wagener FA. Curcumin-induced fibroblast apoptosis and in vitro wound contraction are regulated by antioxidants and heme oxygenase: implications for scar formation. *J cell Mol Med.* 2009 Apr; 13(4):712-25.

23. Jimi S, De Francesco F, Ferraro GA, Riccio M, Hara S. A Novel Skin Splint for Accurately Mapping Dermal Remodeling and Epithelialization During Wound Healing. *J Cell Physiol*. 2016 Sep 14. [Epub ahead of print].
24. Nuutila K, Singh M, Kruse C, Philip J, Caterson EJ, Eriksson E. Titanium wound chambers for wound healing research. *Wound Repair Regen*. 2016 Nov; 24(6):1097-1102.
25. Wang X, Ge J, Tredget EE, Wu Y. The mouse excisional wound splinting model, including applications for stem cell transplantation. *Nat Protoc*. 2014 Feb; 8(2):302-9.
26. Sullivan TP, Eaglstein WH, Davis SC, Mertz P. The pig as a model for human wound healing. *Wound Repair Regen*. 2001 Mar-Apr; 9(2):66-76.
27. Orgill DP and Blanco C (Eds.). 2009. *Biomaterials for Treating Skin Loss*. Sawston, Cambridge, UK. Woodhead Publishing.
28. Trujillo AN, Kesl SL, Sherwood J, Wu M, Gould LJ. Demonstration of the rat ischemic skin wound model. *J Vis Exp*. 2015 Apr 1;(98): e52637.
29. Altavilla D, Saitta A, Cucinotta D, Galeano M, Deodato B, Colonna M, Torre V, Russo G, Sardella A, Urna G, Campo GM, Cavallari V, Squadrito G, Squadrito F. Inhibition of lipid peroxidation restores impaired vascular endothelial growth factor expression and stimulates wound healing and angiogenesis in the genetically diabetic mouse. *Diabetes*. 2001 Mar; 50(3):667-74.
30. Ding J, Kwan P, Ma Z, Iwashina T, Wang J, Shankowsky HA, Tredget EE. Synergistic effect of vitamin D and low concentration of transforming growth

factor beta 1, a potential role in dermal wound healing. Burns. 2016 Sep; 42(6):1277-86.

31. Leslie SK, Cohen DJ, Sedlacek J, Pinsker EJ, Boyan BD, Schwartz Z. Controlled release of rat adipose-derived stem cells from alginate microbeads. Biomaterials. 2013 Nov; 34(33):8172-84.

32. Maxson S, Lopex EA, Yoo D, Danilkovitch-Miagkova A, Leroux MA. Concise review: role of mesenchymal stem cells in wound repair. Stem Cells Transl Med. 2012 Feb; 1(2):142-9.

CHAPTER 4

Conclusion

This thesis has presented multiple studies that indicate the potential of an electrospun and 3D printed cellular delivery device that holds great promise for individualized medicine. Being the first to combine 3D printing with an electrospun biomaterial, this project investigates uncharted territory. Beginning with the design and iterative development followed by in vitro and in vivo experiments, these studies have shown the construct to be capable of supporting cell growth and deserving of continued refinement.

Using techniques of additive manufacturing, the construct was formed through a layered approach. Electrospinning produced a non-woven fibrous mesh mimicking that of the native ECM. This synthetic ECM provided a substrate for cellular growth and formed the base of the cellular delivery device. Alternating layers of electrospun fibers and 3D printed sacrificial elements, an interconnected void space resulted from the dissolution of the sacrificial elements. This novel technique and the utilization of 3D printing allows for nearly any shape to be fabricated to match the needs of a patient, bringing individualized medicine to the treatment of dermal wounds.

Development of the polymer solutions led to the inclusion of polyethylene glycol to improve the electrospinning characteristics. While the incorporation of PEG was able to induce uniform fiber formation, the selection of high molecular weight PEG helped to tailor the degradation characteristics. Low molecular weight PEG created more sites for hydrolysis once dissolved out causing degradation rates that were too fast. Larger

molecules of PEG created fewer gaps in the polyglycolic acid chains, creating a degradation rate that was more appropriate for the wound healing timeline. In vitro degradation proved to be faster in vivo than in vitro which is surmised to be due to cellular enzymatic activity in addition to hydrolysis. Potentially contributing to the slower degradation rate in vitro, the pH of the saline degradation solution was found to be 4.88. This low pH may have inhibited or slowed hydrolysis. Characterization of the construct showed that the diameter of the electrospun fibers were of the proper scale to match that in the established literature. The pore size of the electrospun fibers were also found to be of the appropriate size, small enough to prevent cells from falling through, yet large enough to allow cellular infiltration.

When seeded with mesenchymal stem cells, cultures on constructs exhibited the ability to proliferate while displaying characteristics to suggest a retained stemness. ASCs seeded within the construct were also able to be pushed toward an osteogenic lineage, shown through differentiation markers presented under an osteogenic media treatment.

In vivo, the construct was unable to accelerate wound healing but had no host rejection, a major target and accomplishment for implantable biomaterials. Interestingly, wounds treated with constructs did have significantly higher occurrences of blood vessels within the wound area suggesting the constructs were conducive to angiogenesis. A consistently high level of granulation tissue found in histologic sections of construct treated wounds may be due to possible excipients from the ethanol sterilization process. It is also important to consider the great challenges of the ischemic model, which could not support angiogenesis as the wound be was isolated

from the necessary stem cells in the underlying fascia. Although the construct was sub-optimal in the ischemic model, the *in vivo* studies were among the first to combine the wound splinting and ischemic techniques.

Future work with the electrospun delivery device should focus on the fate of delivered cells. Considering this, *in vitro* work with the constructs could be conducted with a single layer control to better evaluate cell proliferation with respect to provided surface area. *In vivo*, seeded cells could be pre-conditioned to encourage healing and be pushed to further support angiogenesis and host cell migration. A closer examination of the molecular biology of the wound may elucidate cell behavior and fates most supportive of regeneration. The pH of the wound exudate was not considered at the time of *in vivo* experimentation but could provide some insight to the mechanism of degradation and impact of the construct *in situ*. Finally, this construct has great potential to be tailored or modified to include antimicrobial factors, or possibly different factors to be released from each layer of the construct. Ultimately, a perfect incorporation and resorption into the wound will lead to regeneration and remodeling, bridging the gap between injured and normal states.

The concept of individualized medicine is quickly becoming a reality as technology and creativity combine to produce novel treatments with the potential to improve patient outcomes. Although imperfect in the current form, continued advances in engineering and medicine will see novel designs and raw science sculpt the healthcare of the future and help realize the full potential of this work.

REFERENCES

CHAPTER 1

1. Brau RR, Yannas IV. Tissue Engineering of Skin. In: Encyclopedia of Biomaterials and Biomedical Engineering. Marcel Dekker, Inc., New York; 2004. p. 1652-60.
2. Bottcher-Haberzeth S, Biedermann T, Reichmann E. Tissue engineering of skin. Burns. 2010 Jun;36(4):450-60.
3. Lineen E, Namias N. Biologic dressing in burns. J Craniofac Surg. 2008 Jul;19(4):923-8.
4. Boateng JS, Matthews KH, Stevens HN, Eccleston GM. Wound healing dressings and drug delivery systems: a review. J Pharm Sci. 2008 Aug;97(8):2892-923.
5. Russell L. Understanding physiology of wound healing and how dressings help. Br J Nurs. 2000 Jan 13-26;9(1):10,2, 14, 16 passim.
6. Beele H. Artificial skin: past, present and future. Int J Artif Organs. 2002 Mar;25(3):163-73.
7. Langer R, Vacanti JP. Tissue engineering. Science. 1993 May 14;260(5110):920-6.
8. Pomahac B, Svensjo T, Yao F, Brown H, Eriksson E. Tissue engineering of skin. Crit Rev Oral Biol Med. 1998;9(3):333-44.
9. Ramos-e-Silva M, Ribeiro de Castro MC. New dressings, including tissue-engineered living skin. Clin Dermatol. 2002 Nov-Dec;20(6):715-23.
10. Crowther M, Brown NJ, Bishop ET, Lewis CE. Microenvironmental influence on macrophage regulation of angiogenesis in wounds and malignant tumors. J Leukoc Biol. 2001 Oct;70(4):478-90.

11. Jiang W, Schwendeman SP. Stabilization and controlled release of bovine serum albumin encapsulated in poly(D, L-lactide) and poly(ethylene glycol) microsphere blends. *Pharm Res.* 2001 Jun;18(6):878-85.
12. Baker MI, Walsh SP, Schwartz Z, Boyan BD. A review of polyvinyl alcohol and its uses in cartilage and orthopedic applications. *J Biomed Mater Res B Appl Biomater.* 2012 Jul;100(5):1451-7.
13. Ayres C, Bowlin GL, Henderson SC, Taylor L, Shultz J, Alexander J, et al. Modulation of anisotropy in electrospun tissue-engineering scaffolds: Analysis of fiber alignment by the fast Fourier transform. *Biomaterials.* 2006 Nov;27(32):5524-34.
14. Yin A, Zhang K, McClure MJ, Huang C, Wu J, Fang J, et al. Electrospinning collagen/chitosan/poly(L-lactic acid-co-epsilon-caprolactone) to form a vascular graft: mechanical and biological characterization. *J Biomed Mater Res A.* 2013 May;101(5):1292-301.
15. Remya KR, Joseph J, Mani S, John A, Varma HK, Ramesh P. Nanohydroxyapatite incorporated electrospun polycaprolactone/polycaprolactone-polyethyleneglycol-polycaprolactone blend scaffold for bone tissue engineering applications. *J Biomed Nanotechnol.* 2013 Sep;9(9):1483-94.
16. Abd-Allah SH, El-Shal AS, Shalaby SM, Abd-Elbary E, Mazen NF, Abdel Kader RR. The role of placenta-derived mesenchymal stem cells in healing of induced full-thickness skin wound in a mouse model. *IUBMB Life.* 2015 Aug 27.

17. Zheng K, Wu W, Yang S, Huang L, Chen J, Gong C, et al. Bone marrow mesenchymal stem cell implantation for the treatment of radioactivity-induced acute skin damage in rats. *Mol Med Rep*. 2015 Aug 28.
18. Pikula M, Langa P, Kosikowska P, Trzonkowski P. Stem cells and growth factors in wound healing. *Postepy Hig Med Dosw (Online)*. 2015 Jan 2;69(0):874-85.
19. Li H, Duann P, Lin PH, Zhao L, Fan Z, Tan T, et al. Modulation of wound healing and scar formation by MG53-mediated cell membrane repair. *J Biol Chem*. 2015 Aug 25.
20. Rai R, Tallawi M, Frati C, Falco A, Gervasi A, Quaini F, et al. Bioactive Electrospun Fibers of Poly(glycerol sebacate) and Poly(epsilon-caprolactone) for Cardiac Patch Application. *Adv Healthc Mater*. 2015 Aug 13.
21. Steinberg JP, Hong SJ, Geringer MR, Galiano RD, Mustoe TA. Equivalent effects of topically-delivered adipose-derived stem cells and dermal fibroblasts in the ischemic rabbit ear model for chronic wounds. *Aesthet Surg J*. 2012 May;32(4):504-19.
22. Mahjour SB, Fu X, Yang X, Fong J, Sefat F, Wang H. Rapid creation of skin substitutes from human skin cells and biomimetic nanofibers for acute full-thickness wound repair. *Burns*. 2015 Jul 14.
23. Dhall S, Silva JP, Liu Y, Hrynyk M, Garcia M, Chan A, et al. Release of insulin from PLGA-alginate dressing stimulates regenerative healing of burn wounds in rats. *Clin Sci (Lond)*. 2015 Aug 26.

24. Dhall S, Do DC, Garcia M, Kim J, Mirebrahim SH, Lyubovitsky J, et al. Generating and reversing chronic wounds in diabetic mice by manipulating wound redox parameters. *J Diabetes Res.* 2014;2014:562625.
25. Javed F, Al-Askar M, Almas K, Romanos GE, Al0Hezaimi K. Tissue reactions to various suture materials used in oral surgical interventions. *ISRN Dent.* 2012; 212:762095.
26. Cheung H, Lau K, Lu T, Hui D. A critical review on polymer-based bio-engineered materials for scaffold development. *Composites.* 2007; 38:297-300.
27. Baker MI, Walsh SP, Schwartz Z, Boyan BD. A review of polyvinyl alcohol and its uses in cartilage and orthopedic applications. *J Biomed Mater Res B Appl Biomater.* 2012 Jul; 100(5): 1451-7.
28. Lv Q, Guo Q, Han F, Chen C, Ling C, Chen W, Li B. Electrospun Poly(L-lactide)/Poly(ethylene glycol) Scaffolds Seeded with Human Amniotic Mesenchymal Stem Cells for Urethral Epithelium Repair. *Int J Molec Sci.* 2016; 17:1262.